Contribution to the analog simulation of particular dynamic phenomena in rock mass

by

Errol Edward Glasspoole

Dissertation submitted in partial compliance with the requirements for
Masters Degree in Technology
in the
Department of Electrical Engineering (Light Current)
at Technikon Natal.

This Dissertation represents my own work

E.E. Glasspoole

APPROVED FINAL SUBMISSION

24/7/2001

Professor Vladimir B. Bajić, Pr. Eng., D.Eng. Sc.(EE) Date

Supervisor

Acknowledgements

I express my sincere gratitude to Professor Vladimir Bajić for his help, patience and the long hours of discussions which we have shared regarding this project. Without his help, knowledge and encouragement this project would never have been completed.

I also wish to thank Mr. Ron Hacking for his invaluable guidance and patience in the many visits we shared over these topics as well as for reading and guiding me through the many drafts of this dissertation. I also sincerely thank Mr. Carl Reineke for his assistance and knowledge in the origination of the A-D software and for his patience in assisting me in the lab.

Lastly I thank my wife for her everlasting encouragement, understanding and patience, without whom I would not have succeeded.

Contents

Chapter 1

INTRODUCTION

1.1 Background

If a rock mass specimen containing a geological discontinuity (fault) on a slope is subject to increased loading, a point will be reached where the two layers will slide along the discontinuity [11]. The environmental conditions leading to this slip are mostly associated with the rock mass under pressure along the plane of the fault, assuming that this rock mass is practically rigid. Before reaching the point of slide the rock mass is prevented from movement by *friction forces* acting on the discontinuity.

Consider a block of mass m resting on a plane surface which is inclined at an angle θ to the horizontal. The block is acted on by gravity only and hence the gravitational force ($F = mg$) acts vertically downwards as shown in the diagram below. The resolved part of F which acts down the plane and which tends to cause the block to slide is $mg \sin \theta$. The component of F which acts across the plane and which tends to stabilise the slope is $mg \cos \theta$.

The rock mass will begin to move once the shear stress has overcome the shear force R.

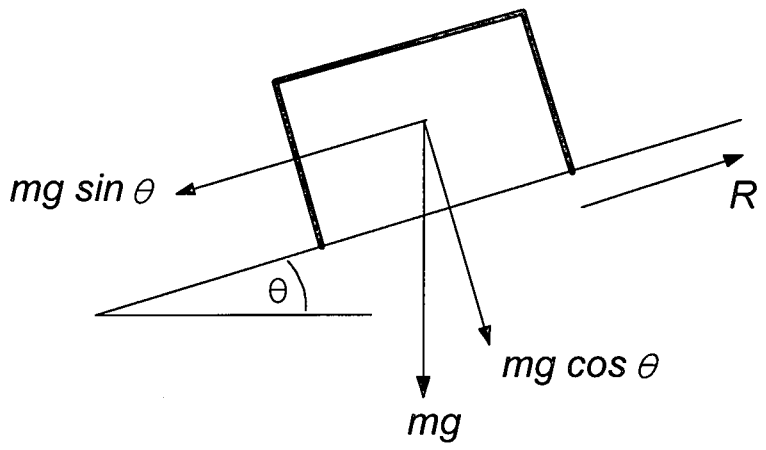

Figure 1

When force is applied to an object it is said to be under **stress**. The stress may be **compressive**, tending to squeeze or compress it, or it may be **tensile**, tending to pull the object apart. A shearing stress is one that tends to cause different parts of the object to be displaced across a plane, or to slide past one another [11].

Strain is deformation - a change in the shape, volume, or both - resulting from stress. It may be either temporary or permanent, depending on the amount and type of stress and the material's strength to resist it. If the deformation is **elastic**, the material returns to its original size and shape when the stress is removed. Rocks also have the ability to behave elastically, although much greater stress is needed to produce detectable strain. Once the **elastic limit** of a material is reached, the material may go through a phase of **plastic deformation** with increasing stress. During this stage relatively small added stresses yield large corresponding strains, and the changes of shape are permanent. Once in this state the material does not return to its original dimensions after removal of the stress.

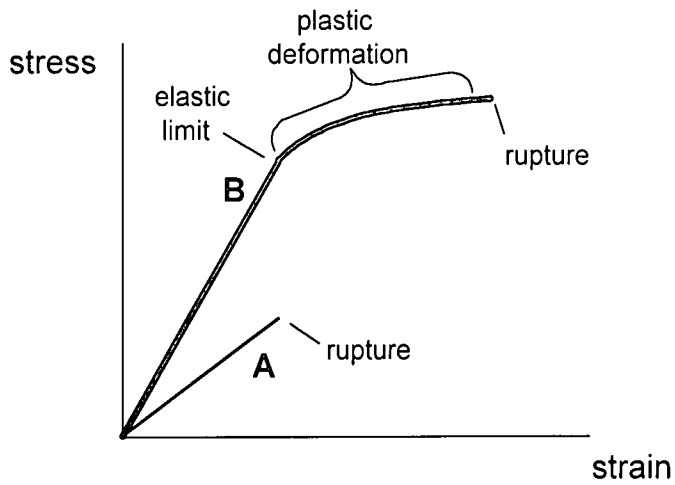

Stress - Strain relationship

A : for brittle materials

B : for materials capable of plastic deformation

Figure 2

Failure or breakage occurs when stress exceeds rupture strength.

Hooke's law states that a given strain is linearly proportional to the stress producing it. When applied to an isotropic medium (one whose properties do not depend on direction), a resistance to shearing strain develops. For a given substance when the stress is increased beyond the elastic limit, Hooke's law no longer holds and the strains increase more rapidly for a given change in stress. Strains resulting from stresses which exceed this limit do not entirely disappear when the stresses are removed, ie; the material behaves plastically.

If stress is increased further, solids eventually break, or **rupture**. In **brittle** materials, rupture may occur before there is any plastic deformation. Brittle behaviour is characteristic of most rocks at near-surface conditions. At greater depths, where temperatures are higher and rocks are confined (in a sense, supported by rocks at high pressure), rocks may behave plastically, as they do in an asthenosphere. Plastic deformation of rocks deep in the crust is often reflected in the production of folds; brittle behaviour yields **faults**, resulting from planar breaks in rock along which there is movement of rocks on one side relative to rocks on the other.

Major earthquakes demonstrate dramatically that the earth is a dynamic, changing system. They can occur along existing faults, or may be related to formation of new ruptures in rock under stress. When friction between rocks on either side of a fault is such as to prevent the rocks from slipping easily, or when the rock under stress is not already fractured, some elastic deformation occurs before failure. When the stress exceeds the rupturing strength of the rock (or the friction between the rocks along an existing fault), sudden movement occurs; resulting in an **earthquake**.

The stressed rocks released by the rupture, snap back elastically to their previous dimensions, a phenomenon fundamental to earthquake mechanics, known as **elastic rebound**, first described by the investigator of the 1906 San Francisco earthquake, Harry Fielding Reid [26]. The occurrence of movement and stress release is reflected in displacement of the rocks on either side of the fault following the earthquake, often in a cyclic wave fashion.

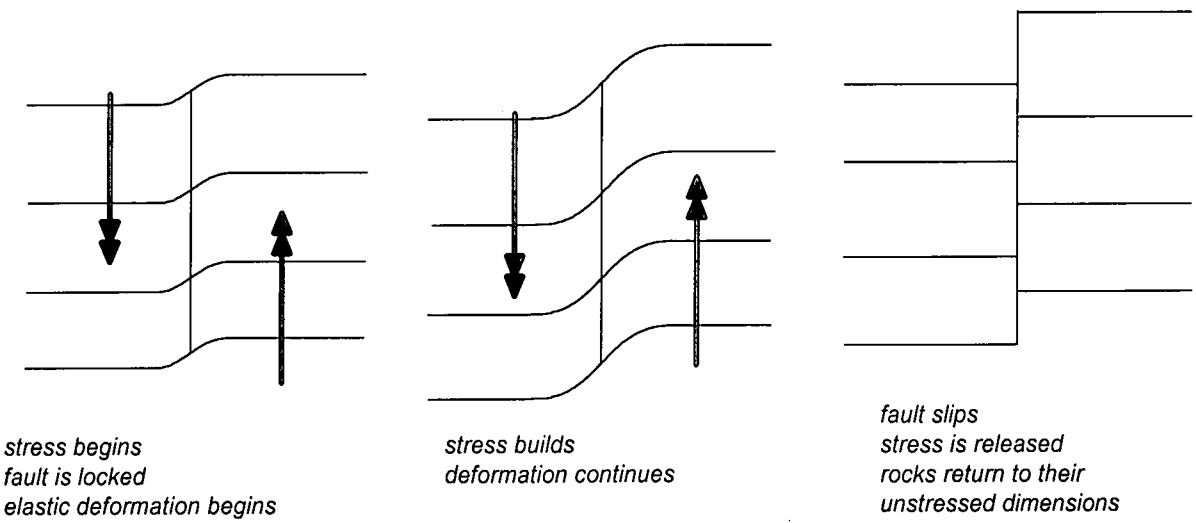

The phenomenon of elastic rebound along a fault zone.
The rocks deform elastically under stress until failure, then snap back to their original, undeformed condition after the earthquake.

Figure 3

Body waves

The stored energy released during an earthquake travels away from the focus in the form of seismic waves. There are several types of seismic waves, the predominant being what are called **body waves** (P-waves and S-waves) which travel through the interior of the earth and **surface waves** which travel along the surface. Newton's second law of motion [26] states that "*the unbalanced force equals the mass times acceleration*" and from this a wave equation of motion along a longitudinal *x*-axis can be developed. This *wave* can be seen as a "disturbance" which travels through the medium and, being a wave, its geometric aspects can be considered [17]. The simplest form of time varying wave is the harmonic wave which has a simple harmonic motion and which can be analysed in terms of its amplitude, wavelength, period and frequency.

P-waves are also known as longitudinal, compressional or simply *primary* waves as they are usually the first event on an earthquake recording; ie. they move faster than shear or surface waves. P-waves are the dominant waves involved in seismic exploration. As P-waves travel through matter they produce forces which alternately compress the particles of rock in front of the movement and expand those behind it. The rock particles adjust to this motion and allow a series of pulsations to move out in all directions away from this event.

S-waves are shear waves, involving a side-to-side sliding motion of the material, lateral to the direction of propagation. P-waves travel faster through rock than S-waves, at speeds of up to 6 kilometres per second.

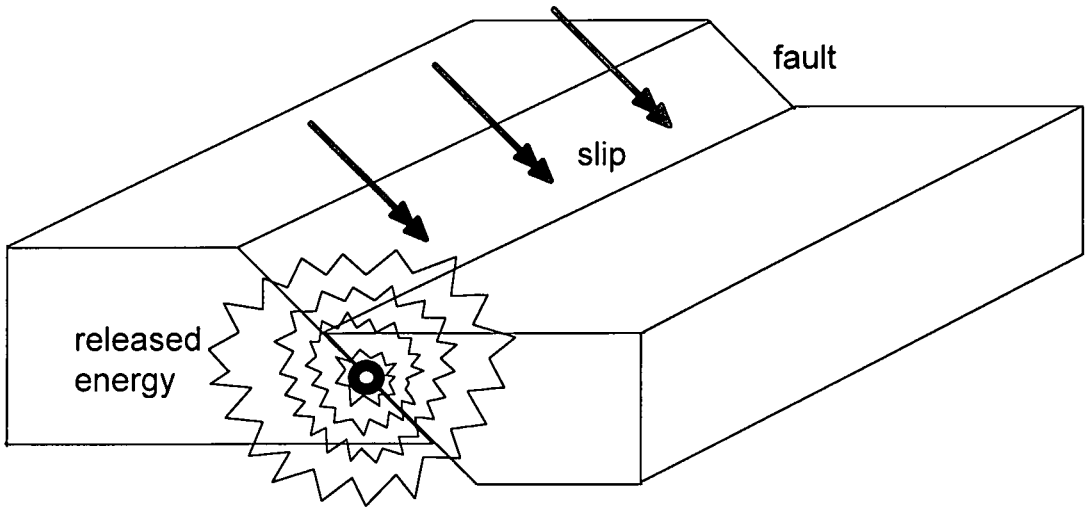

Figure 4

Development of a Mechanical Model of Rock Mass Sliding

A simple mechanical model for considering earthquake faults was developed by Burridge and Knopoff [2] some thirty years ago. This model received wide acclaim and it formed the basis for many projects studying earthquake behaviour [7], [14]. During intensive simulation of the Burridge-Knopoff model a particular occurrence of sudden unpredictable release of energy became apparent as observed by Carlson & Langer [7].

This chaotic release of energy took place in spite of the model under test being predictable (deterministic). Hence, even as the model appeared at first stable this sudden release of energy indicated a hidden chaotic behaviour resulting from a type of chain response [1] of the "avalanche type" which occurred during specific stimulus conditions. This chaotic unpredictable system behaviour can only be explained as a result of non-linearities existing in the model. In an adaptation of the Burridge-Knopoff model evaluated by Carlson & Langer [7], the only non-linear component of the model was the friction law of the so called "stick-slip" type which is velocity dependent.

Bajić [1] originated a pilot study in which a similar model type was used to simulate the behaviour of rock mass. His initial assumption was that many underground dynamic conditions can be described on the basis of both Newton's laws and a nonlinear "stick-slip" friction law and that these two laws would be adequately suitable for modelling the realistic behaviour of the rock mass. Bajić surmised that this approach would also reveal the chaotic energy releases which were observed in the Carlson & Langer studies. His study concentrated on investigating this chaotic "chain reaction" release of energy under certain defined conditions. He further surmised that if the "chain reaction" could be observed in the model, then it was likely that similar situations may occur in real situations leading to rock material fracture or even rock bursts. He proposed that a further useful outcome of such an analysis could reveal a simple time dependence relationship of the kinetic energy released. Such a model could be considered as a one dimensional "line" model emanating in one direction from the source of the seismic wave. He concluded that this approach could serve as a complementary tool to the elasto-dynamic model approach to simulate rock mass behaviour [9], [16].

As the actual mechanism of rock bursts has not yet been fully explained Bajić's study was an effort to contribute to explanation of this phenomenon. The model type he used was based on a digital computer.

1.2 Motivation for research

The aim of this project is to develop an analogue computer model for simulation of dynamic behaviour of rock mass. This design should be modular to allow easy change of the order of simulated model.

It is hypothesized that the system developed will, in principle, produce a simulation time which is considerably less dependent on the change of order of the model than is the case with simulation on a digital computer. In addition, the proposed simulation approach will be independent of the type of numerical integration, since no numerical integration is used in analog simulation structures.

Thus the proposed project will solve both problems noted above which are associated with the use of a digital computer based simulation approach. It is not the task of the project to develop a commercially suitable analog computer for the above purpose but to show that, by use of analog simulation techniques, the previously indicated problems could be considerably reduced.

Upon analyzing the problem, the following three sub-problems have been identified:

i. Development of an analog network consisting of separate cells (with each cell representing a number of cells in the mechanical ladder network) which will model the mechanical ladder network used by Bajić (1992); this analog modeling will allow the simplified change of the order of the model;

ii Design of a suitable data acquisition system which will sequentially scan and interpret data from a large number of sources (where sources are various nodes in the simulation network);

iii Correct selection of the format necessary for the presentation and storage of data in the memory of a digital computer.

1.3 Delimitations

It is envisaged that the following delimitations will adequately determine the scope of the project:

i. This study will not attempt to develop a commercially suitable analog computer but merely to investigate the possibility that, in principle, the proposed approach based on the analog simulation technique, will considerably reduce the previously indicated problems.

ii. This project will not be involved with the problems concerned with the processing of the measured data stored in the computer memory, but will stop at the point at which data is stored in memory.

1.4 Assumptions

In the project the following general assumptions are made:

1. The mathematical-mechanical model described by Carlson & Langer [7] was developed for specific dynamic phenomena. It is assumed that the results obtained by Bajić [1] are both valid and accurate.

2. It is assumed that the characteristics and tolerances (physical values of parameters) of the components selected for use in the construction of the analog model and the data acquisition system, will be sufficiently precise and stable so as to function properly.

3. Actual simulations (of later defined Types 1, 2 and 3) are merely to verify the correctness of the analogue model. These will also be used to see if this simple 1-D model can be further generalised to 2-D and 3-D so as to simulate real-world conditions such as those in deep-level mines.

Chapter 2

COMPUTER SIMULATION

2.1 Development of the 1-D model

The Carlson-Langer model was developed under boundary conditions that describe the effects on a body existing on the earth surface. The Bajić variant of this model changed these boundary conditions by assuming an underground situation where the body was surrounded by a solid rock mass. The Bajić model was essentially one dimensional consisting of a series of cells each coupled together as well as to the surrounding rock mass. The equations developed to express the velocity effects of this series of blocks were therefore one dimensional.

2.2 Model variants

The one dimensional wave equation (a partial differential equation) was considered by Carlson and Langer [7] and compared to the variant of the Burridge-Knopoff model they used. Their deduction was that the two approaches showed no direct equivalence under certain conditions. This was due to the fact that some of the parameters in the wave equation tend to infinity in the limit process thus the defining wave equations could not be derived from the model under consideration. The discrepancies in the tests arose under the conditions when the sizes of each individual cell was reduced to zero. Thus a proper equivalence of models was not obtainable.

However through a series of experiments Bajić [1] was able to show that a similarity does exist. Although such evidence did not confirm a direct equivalence it rather indicated that, for certain types of dynamic phenomena, the precise differences between the models could be properly posed and explained. In this way the validity of the Burridge-Knopoff types of model could be assessed. Bajić's project studied the Carlson-Langer variant of the Burridge-Knopoff model which was a purely mechanical approach, taking into account Newton's laws, developed for surface conditions. He then re-defined the initial conditions for an underground situation including the non-linear "stick-slip" situation. The aim of the model was to simulate the dynamics of a part of the rock mass, highlighting these dynamic effects and neglecting other non-dynamic micro-phenomena occurring during the event such as the change in the rock structure. The elastic properties of the material are modelled through the stiffness coefficients of the springs used in the model.

Because of its simplicity and the great number of effects which the model could display it was found useful for qualitative investigation of some seismic events. Bajić also found that his model was suitable for a reasonably fast simulation.

He took the Carlson-Langer model and changed the spacial boundary conditions and the temporal initial conditions to simulate an underground situation. His aim was to try to simulate the conditions leading to the appearance of the sudden weakening of the material on the plane of weakness in the rock mass and to observe these effects on the individual components of the rock mass. His hypothesis was that this could be considered as the situation existing when new fractures appear in the rock mass.

2.3 Model tests

Bajić conducted three types of simulational experiments.

The first type, aimed at trying to produce a "violent" chaotic reaction, was run under the "standard" conditions and the effects closely monitored and observed.

The second type experiment aimed at studying the effects of a sudden reduction of static friction at different positions in the sequence of blocks.

The third type experiment aimed at a simulated case of water being pumped under high pressure into a fault, with the results also recorded.

A "chain" reaction was observed between the motions of the blocks under test, see Appendix #1 (p 54) from [1] and it was therefore deduced that further more sophisticated experiments could generate other interesting effects. The aim was to hopefully simulate the wild chaotic system response which was originally aimed for study. These results also indicated that more advanced 2-D and 3-D models would reveal further detailed insight into the behaviour of rock mass layers.

A problem Bajić encountered with this model was that of "scaling". This entailed relating the actual physical values under test with the model parameters and he correctly surmised that the solution of this problem when applied to a 2-D or 3-D model would also yield more accurate and realistic results.

Due to the difficulties mentioned, the present model could serve mainly as a subsidiary tool for the analysis of dynamic phenomena of a rock mass, which is more of a qualitative than a quantitative nature. In any case, the model should be considered only as a complementary one with the already existing elastodynamic models for rock mass behaviour.

Computer programme developed

After intense study of the Burridge-Knopoff model a phenomenon which was not directly predictable was observed. This concerned the sudden release of energy which pointed to a hidden chaotic type of system behaviour which was evident in a chain-response of an avalanche type as discovered by Bajić [1] under specific conditions. This non-linear behaviour was the result of non-linearities being introduced into the system model.

The Carlson-Langer variation of the model considered the friction law to be the non-linear element which was velocity dependent and of the "stick-slip" type. Bajić's study developed a similar model for simulation of behaviour of a rock mass but on considerably different conditions - rock mass layers deep below the surface slipping relative to each other.

Advantages of the study

The useful consequences of this study were:

i The study concentrated on the investigation of the "chain" reaction under specific circumstances. If this reaction could be noticed in the simulation, this could be imagined to reflect situations occurring in rock material fractures or even a rock burst. Actually, such phenomena are observed in mining practice.

ii The simple calculation of time evolution of the potential energy exhibited in simulated events.

iv. The study could also be considered as a rough simple "line" model for the source of seismic waves experienced in mining practice.

This was proposed to serve as a complementary tool to the approach based completely on elastodynamic models of Domingues & Alarcon [9] and Mansur & Brebbia [16].

2.4 Problems identified with the model

In his study Bajić showed that particular dynamic phenomena in rock mass could, to some extent, be simulated by a digital computer. He identified two main problem areas which appeared with respect to this approach:

i. **The order of the model**

Since the problem involved is naturally distributed in space it is properly described with partial differential equations. Simulation of these equations on digital computers is based on the approximation given as a set of ordinary differential equations. The quality of such approximation is directly associated with the order of the approximation model. To improve the approximation the order of the model has to be sufficiently high. As a consequence the required simulation time will be increased. For example, if the rock mass layer model is simulated by a chain of n blocks, the associated approximation model is of order 2n. Hence the larger n the longer will be the simulation time.

ii. **Integration method**

The selection of the method for integrating the differential equations of the model also affects the simulation time. Different integration methods require different step size for sufficiently accurate integration, which again directly influences the required time for integration (and hence simulation time).

Chapter 3

Analogue Model

3.1 Background to computer modelling solutions

A system can be represented by a schematic block diagram with each block representing the relevant input-output relationship of the block. A model of a complex system can comprise a larger block diagram with a number of elements each with relatively simple input-output characterisation of the blocks. Such a system, if it is linear and time- invariant, can be reduced to a single block with a higher order transfer function relating the system's output to its input.

In principle there are two computer solution methods used to achieve quick system response. These are:

i a digital solution using some form of high level simulation language,

ii an analogue computer solution.

A digital computer is a discrete data machine which operates normally in a serial mode. Although it is a highly sophisticated calculating machine performing simple arithmetic operations sequentially at very high speeds, real time simulations may not always be possible. Such a machine makes it possible to arrive at extremely accurate solutions, however often at the expense of long computational times.

An analogue computer is a machine in which a range of physical, discrete components are connected to model the equations describing the physical behaviour of the system to be studied. The analogue system is then directly comparable to the real time physical system. The analogue computer is a continuous data device operating in a ***real time parallel mode***.

During operation the electronic analogue computer can be interrogated at any of its circuit nodes to yield a range of voltages, each reading representing the values of a variable that enters the system model description [22]. Thus the electronic analogue computer is particularly suitable for the solution of differential equations and hence for the simulation of dynamic systems [23] such as the equations that describe the behaviour of the moving rock mass systems above.

3.2 Development of a 1-D analogue computer model

The project aim is to develop an analogue computer model which can simulate the dynamics of two rock mass layers moving with respect to each other.

- The proposed model studied a chain of "n" blocks each with a mass m_j where $j = 1, 2, \ldots\ldots, n$.
- Coefficients k_S and k_P roughly represent elastic properties of the contact region with respect to compression (k_S), and with respect to shear (k_P). The junctions between the blocks as well as to the surrounding rock mass are represented by coefficients that are properties of compression "k_s" and leaf spring "k_p". Each coefficient represents some form of elastic property.
- The blocks are joined by springs each with a stiffness coefficient k_s. Hence the j *th* block and the $(j\text{-}1)_{th}$ block are coupled by a spring with a coefficient k_s^j . Also as the end spring appears between the n *th* block and the surrounding rock mass not corresponding to any particular block used in the model, its stiffness coefficient is k_s^{n+1} .
- Each block is coupled to an immobile surface by a "leaf spring" (or torsion element) having a coefficient of k_p. Hence the stiffness coefficient of the "j_{th}" block is denoted by k_p^j .
- All blocks rest on a surface which may move during some time intervals. This moving surface is assumed to be rough and friction forces arise between it and the blocks. The speed of the moving surface is v.

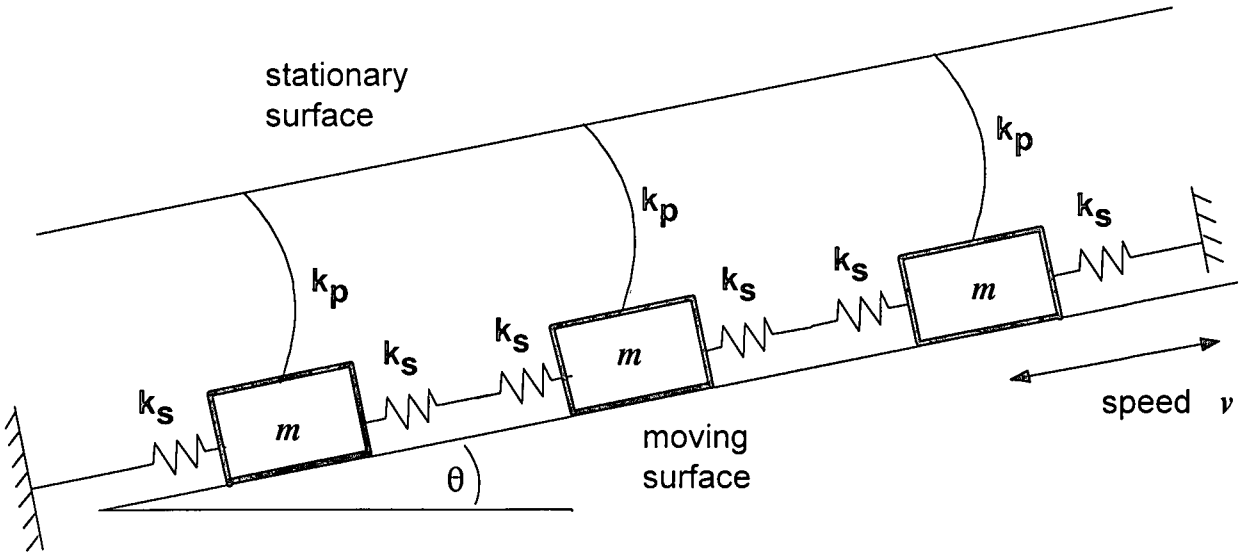

Figure 5

3.3 Initial equations developed to represent each block

The model for the system described in Fig. 5 is developed in [1].

The basic premise was that, in principle, two "states" are possible for each block: the block can move with respect to the moving surface, or, under certain conditions, it will not move with respect to the moving surface [6].

3.3.1 Dynamic equations of the model

The movement of each block is time dependant. A block moves in some time intervals according to the specific conditions to which it is exposed [18].

Let $D = \frac{d}{dt}$ denote the ordinary derivative with respect to time t, so that $\dot{x} = D\,x$.

The equation of dynamics for each block is based on the analysis of forces [13] that act on the j th block. This holds while the block moves (relative to the moving surface):

$$m_j D^2 x_j = k_s^{j+1}(x_{j+1} - x_j) - k_s^{j} (x_j - x_{j-1}) - k_p^{j} x_j + (W_j + m_j g) \sin\theta - F_j \qquad j = 2, 3, \ldots, n-1$$

$$m_1 D^2 x_1 = k_s^{2} (x_2 - x_1) - k_2^{1} x_1 - k_p^{1} x_1 + (W_1 + m_1 g) \sin\theta - F_1 \qquad j = 1$$

$$m_n D^2 x_n = -k_s^{n+1} x_n - k_s^{n} (x_n - x_{n-1}) - k_p^{n} x_n (W_n + m_n g) \sin\theta - F_n \qquad j = n$$

Here F_j, $j = 1, 2, \ldots, n$ represent a velocity dependent friction force between the j th block and the moving surface and W_j is the vertical force acting downwards on the j th block.
Variable x_j represents the displacement of the j th block with respect to its initial position.

These three equations are then converted into the following simple forms so as to be used in developing an active cell model as part of an analogue simulation system.

The equations describe the three forms of block which are found in the model.

These are:

Block 1: (the first block : j = 1)

$$j = 1: \quad m_1 x_1 = k_s^2 (x_2 - x_1) - k_s^1 x_1 - k_p^1 x_1 + (W_n + m_1 g) \sin\theta - F_1$$

Block 2: (the intermediate block (or blocks) : j = (n-1), (n-2), (n-3), ... , (n-x))

$$j = (n-1): \quad m_j x_j = k_s^{j+1} (x_{j+1} - x_j) - k_s^j (x_j - x_{j-1}) - k_p^j x_j + (W_j + m_j g) \sin\theta - F_j$$

Block 3: (the last block in the chain : j = n)

$$j = n: \quad m_n x_n = k_s^{n+1} x_n - k_s^n (x_n - x_{n-1}) - k_p^n x_n + (W_n + m_n g) \sin\theta - F_n$$

These equations were then multiplied out to yield:

$$j = 1: \quad m_1 x_1 = k_s^2 x_2 - k_s^2 x_1 - k_s^1 x_1 - k_p^1 x_1 + (W_n + m_1 g) \sin\theta - F_1$$

$$j = (n-1): \quad m_j x_j = k_s^{j+1} x_{j+1} - k_s^{j+1} x_j - k_s^j x_j + k_s^j x_{j-1} - k_p^j x_j + (W_j + m_j g) \sin\theta - F_j$$

$$j = n: \quad m_n x_n = k_s^{n+1} x_n - k_s^n x_n + k_s^n x_{n-1} - k_p^n x_n + (W_n + m_n g) \sin\theta - F_n$$

Here:

F_j = velocity dependent non-linear friction force between the j th block and the moving surface.

W_j = vertical force acting downwards on the j th block.

x_j = displacement of the j th block.

m_j = mass of the block.

k_s = spring stiffness coefficient - mutually coupling each block.

k_p = lateral leaf spring element coefficient - coupling each block to the stationary surface.

k_s and k_p : are both elastic properties of the contact region with respect to: compression - k_s

shear - k_p

Note: these two terms are labelled as *coefficients* as the deflections are regarded as negligibly small and hence this is a piecewise-linear model.

v = speed of the moving surface.

g = gravitational acceleration.

v_i = velocity of block relative to the moving surface.

$(w_n + m_1 g) \sin\theta$ = a constant relating to the angle of the surface on which the blocks rest.

x = displacement $\quad \dot{x}$ = velocity $\quad \ddot{x}$ = acceleration

3.3.2 Converting equations into a suitable format for analog modelling

Each equation, beginning in its dynamic form is transformed into its kinematical form (equation of motion). They are each first simplified and then normalised [25]. In this process the parameter values used in [1] are applied. These are;

rock mass	m is 10^{10} kg.
spring stiffness coefficient	k_s is 10^{11} kN/m.
lateral leaf spring element coefficient	k_p is 10^{9} kN/m.

Block 1: j = 1

$$m_1 \overset{\circ\circ}{x}_1 = k_s^2 x_2 - k_s^2 x_1 - k_s^1 x_1 - k_p^1 x_1 + (w_1 + m_1 g)\sin\theta - F_1$$

$$\overset{\circ\circ}{x}_1 = \frac{k_s^2}{m_1}x_2 - \frac{k_s^2}{m_1}x_1 - \frac{k_s^1}{m_1}x_1 - \frac{k_p^1}{m_1}x_1 + \frac{(w_1 + m_1 g)}{m_1}\sin\theta - \frac{F_1}{m_1}$$

$$= \frac{(10^{11})}{10^{10}}x_2 - \frac{(10^{11})}{10^{10}}x_1 - \frac{(10^{11})}{10^{10}}x_1 - \frac{(10^{9})}{10^{10}}x_1 + \frac{(w_1 + m_1 g)}{10^{10}}\sin\theta - \frac{F_1}{10^{10}}$$

$$\overset{\circ\circ}{x}_1 = 10x_2 - 10x_1 - 10x_1 - 0{,}1x_1 + \frac{(w_1 + m_1 g)}{10^{10}}\sin\theta - \frac{F_1}{10^{10}}$$

Block 2: j = (n-1)

$$m_j \overset{\circ\circ}{x}_j = k_s^{j+1}x_{j+1} - k_s^{j+1}x_j - k_s^j x_j + k_s^j x_{j-1} - k_p^j x_j + (w_j + m_j g)\sin\theta - F_j$$

$$\overset{\circ\circ}{x}_j = \frac{k_s^{j+1}}{m_j}x_{j+1} - \frac{k_s^{j+1}}{m_j}x_j - \frac{k_s^j}{m_j}x_j + \frac{k_s^j}{m_j}x_{j-1} - \frac{k_p^j}{m_j}x_j + \frac{(w_j + m_j g)}{m_j}\sin\theta - \frac{F_j}{m_j}$$

$$= \frac{(10^{11})}{10^{10}}x_{j+1} - \frac{(10^{11})}{10^{10}}x_j - \frac{(10^{11})}{10^{10}}x_j + \frac{(10^{9})}{10^{10}}x_{j-1} - \frac{(10^{9})}{10^{10}} + \frac{(w_j + m_j g)}{10^{10}}\sin\theta - \frac{F_j}{10^{10}}$$

$$\overset{\circ\circ}{x}_j = 10x_{j+1} - 10x_j - 10x_j + 10x_{j-1} - 0{,}1x_j + \frac{(w_j + m_j g)}{10^{10}}\sin\theta - \frac{F_j}{10^{10}}$$

Block3: j = n

$$m_n \overset{\circ\circ}{x}_n = -k_s^{n+1}x_n - k_s^n x_n + k_s^n x_{n-1} - k_p^n x_n + (w_n + m_n g)\sin\theta - F_n$$

$$\overset{\circ\circ}{x}_n = -\frac{k_s^{n+1}}{m_n}x_n - \frac{k_s^n}{m_n}x_n + \frac{k_s^n}{m_n}x_{n-1} - \frac{k_p^n}{m_n}x_n + \frac{(w_n + m_n g)}{m_n}\sin\theta - \frac{F_n}{m_n}$$

$$= -\frac{(10^{11})}{10^{10}}x_n - \frac{(10^{11})}{10^{10}}x_n + \frac{(10^{11})}{10^{10}}x_{n-1} - \frac{(10^{9})}{10^{10}}x_n + \frac{(w_n + m_n g)}{10^{10}}\sin\theta - \frac{F_n}{10^{10}}$$

$$\overset{\circ\circ}{x}_n = -10x_n - 10x_n + 10x_{n-1} - 0{,}1x_n + \frac{(w_n + m_n g)}{10^{10}}\sin\theta - \frac{F_n}{10^{10}}$$

Upon isolating the simplified versions of the three equations (as summarised below) it is evident that they are similar in many respects.

$$\ddot{x}_1 = 10x_2 - 10x_1 - 10x_1 - 0{,}1x_1 + \frac{(w_1 + m_1 g)}{10^{10}} \sin\theta - \frac{F_1}{10^{10}}$$

$$\ddot{x}_j = 10x_{j+1} - 10x_j - 10x_j + 10x_{j-1} + \frac{(w_j + m_j g)}{10^{10}} \sin\theta - \frac{F_j}{10^{10}}$$

$$\ddot{x}_n = -10x_n - 10x_n + 10x_{n-1} - 0{,}1x_n + \frac{(w_n + m_n g)}{10^{10}} \sin\theta - \frac{F_n}{10^{10}}$$

Each equation represents the sum of similar terms [25]:

a number of terms, each representing a function of displacement: (x)

one term being a constant: $(w_1+m_1 g)\ sin\ \theta$

one term being the velocity dependent friction force which is non-linear: (F_j)

When added together these terms all produce the second derivative of displacement: (x)

namely acceleration : $(\ddot{x})$

Apart from a few "minus" signs and one or two terms differing in value by the order of magnitude or two, these three equations can all be modeled by a similar, single circuit model.

3.4 Scaling

One problem in analog simulation may be that we want to observe the system response in a different time scale than when it is normally obtained. Also, for any given input signal the maximum values of the voltage signals within the circuit, which depend on the maximum values of each variable and its derivatives, must be neither too large that the linear range of one or more of the amplifiers is exceeded, with resulting errors in the solution, or so small that poor signal-noise ratios cause unacceptable inaccuracy.

Modification to a circuit diagram to minimize these problems takes two forms referred to as ***time scaling*** where the solution is time altered and ***magnitude scaling*** (or ***amplitude scaling***) where the variables are scaled to ensure that voltage levels throughout the circuit are as high as possible without exceeding the reference values [18], [22].

Inspection of the system coefficients and the gain values in the circuit diagram will often suggest whether or not scaling is likely to be needed, perhaps requiring suitable modification.

For any electronic analog computer model variables are directly proportional to the problem variables in such a way that α volts (for example) represent one unit of the corresponding variable. The magnitude of the forcing function voltage can then be increased so that the operating voltages within the circuit become as large as possible without anywhere exceeding the reference voltage and preferably until the scaling constant is a convenient number.

Provided that the problem solution time is reasonable and that voltages are not so small that unacceptable errors are likely to occur then no further action on scaling is required.

Magnitude Scaling

In order to arrange each of the individual circuit components to vary between similar supply rails and be each of a similar magnitude a ***magnitude scaling factor*** is introduced.

The magnitude of the output voltage of the circuit depends a great deal on the circuit's accuracy. In setting up the circuit the operating voltage limit lies between ± 10 V.

Since the analogue computer circuit manipulates voltages, it is necessary to transform the real system equations which involve displacement to analogous voltage equations. Thus the displacement [x] is represented by a voltage value and the magnitude scale factors relate the amplifier's output voltages to the corresponding physical quantities being modelled.

To avoid saturation a scale factor is used which keeps the operating voltage between the allowed limits. If this is not done *voltage saturation* will cause errors in the solution. Also, to eliminate random noise effects and to ensure maximum accuracy, the maximum supply voltage is made as large as possible.

The first step in determining magnitude scale factors is to estimate the maximum magnitudes of variables that will occur in the physical system. In practice variable ranges are usually unknown before the solution is obtained. Such estimates may come from a knowledge of the actual system or rough estimations.

Once the initial estimates of the maximum magnitudes of variables are found, magnitude scale factors can be determined.

For this specific circuit the scaling factors were arrived at in the following manner:

1. The first consideration involves limiting the range of the voltage supply to the selected op amp devices. This was set at a maximum output of ±10 V.
2. Each multiplier in the model was chosen to produce a standard maximum gain of ten which simplified circuit design.

In a practical design note, the possibility of exceeding supply voltages was considered, so to eliminate any possible infringement into a saturation area, the amplifiers of each multiplier were designed with a variable gain capability.

3.5 Analogue computer model solution to the differential equation

After magnitude scaling the equations are finally in a form which allows for each term to be modeled by an equivalent analogue circuit.

All the terms in the three equations are similar; thus a single circuit has been developed which is capable of modeling all three equation types with only slight modifications, so as to exactly model each specific equation.

The generalized equation is arranged with its highest derivative term forming one side of the equation and all the other subsequent terms arranged in order forming the opposite side of the equation. This is done in order to develop a logical analogue model of the system, the right hand terms all arranged to form the total sum of the highest derivative.

General equation form: $$m\ddot{x} = k_s^2(x) - k_s^1(x) - k_p(x) + (y)\sin\theta - F$$

This equation will be used to develop a master cell.

Summing amplifier

To create the sum total of all of the terms (which ultimately represents the acceleration $\ddot{x}$) each of the signals are introduced simultaneously to a summing amplifier [5], [18]. Each of the signals fed into this amplifier represents either feed-back or feed-forward terms appearing in the right hand sum of the generalised equation as given above. The output of this block represents the acceleration $\ddot{x}$ as appearing on the left of the generalised equation above. This sum total acceleration produces the highest derivative term at the point in the circuit as required [21]. The summing amplifier is depicted in Fig. 6.

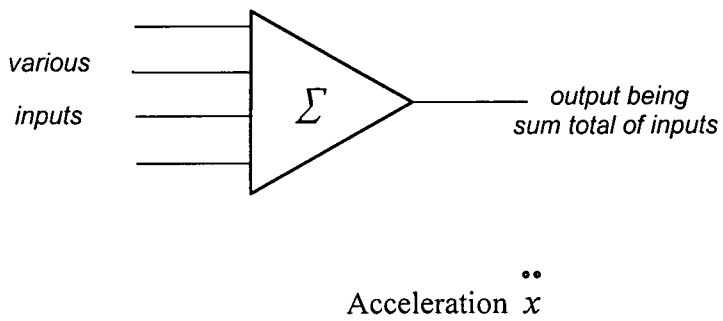

Figure 6

Integration

As the system's input ($\ddot{x}$) represents the highest derivative term in the equation, then lower derivative terms can be obtained by successive stages of integration [5], [10]. Therefore in the circuit model two successive blocks of integration are necessary (Fig. 7) in order to achieve the necessary outputs as required by the master cell equation [18], [21]. The input to the first integrator corresponds to acceleration $\ddot{x}$ which, when integrated, produces a voltage that corresponds to the velocity and when again integrated produces the displacement.

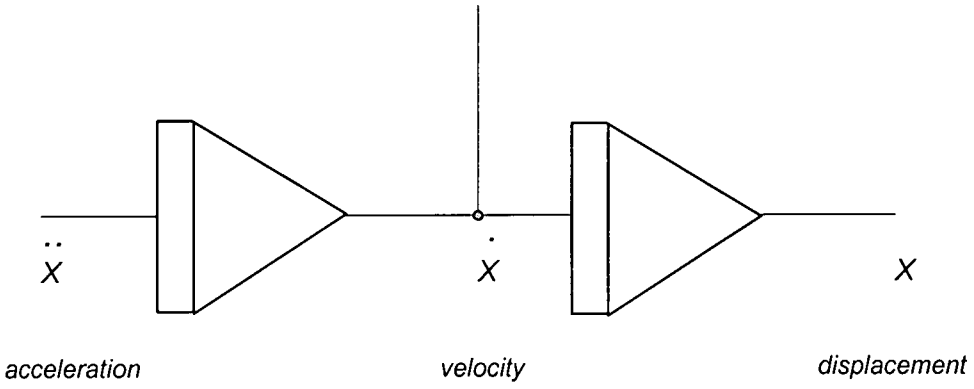

Two Successive Stages of Integration

Figure 7

3.5.1 Circuit modelling

The procedure for modelling an equation is as follows [25];

i estimate the maximum values for each variable $x_r(t)$, for the forcing function of interest,

ii determine scaling factors, which are equal to or slightly less than the corresponding ratio $\dfrac{reference\ \ voltage}{maximum\ \ expected\ \ value\ \ of\ \ x_r(t)}$.

iii re-write the differential equations in terms of their scaled variables.

iv draw the circuit diagram.

v construct and test the circuit, observe maximum voltages throughout and readjust where necessary.

3.6 Non-linear circuit

The analogue computer is particularly useful for simulating systems where non-linearities are present such as in this particular application. It was necessary here to implement a system which would model the non-linear "stick-slip" effect inherent in the mathematical model in both the positive as well as the negative direction of rock mass block movements.

The "stick-slip" phenomenon

This phenomenon occurs when a force is exerted onto a body which, in reply, does not immediately respond. As the applied force rises the friction between the body and the resting surface keeps the body from moving. Finally a point is reached where the applied force rises to a level that exceeds the friction force and the body "slips" and there is a corresponding increase in velocity of the body while at the same time the applied force falls. This event causes a non-linear, decreasing response as, with an increasing velocity the applied force falls.

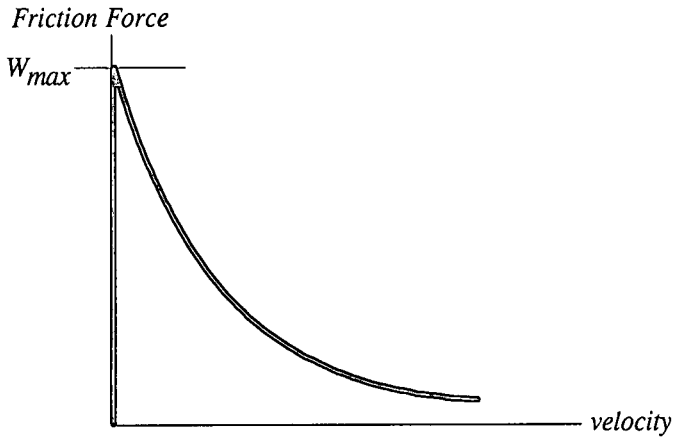

Figure 8 *Non-linear characteristic of the "stick-slip" phenomenon*

The non-linear "stick-slip" circuit

Although a number of standard elements were considered, for example servo multipliers or diode function generators, these do not offer a satisfactory solution to this circuit's requirements as they each have a fixed, unvariable characteristic which also extend in only one direction, not "mirrored" in the reverse direction. It was necessary to design a unique discrete analogue circuit to create the non-linear "stick-slip" effect required with optional variable inputs available. This circuit, referred to as the "non-linear cell", is represented in the master cell circuit diagram by the symbol shown below;

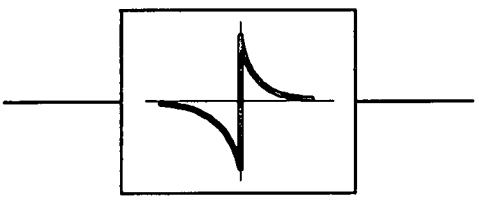

non-linear cell symbol

Figure 9

The non-linear cell represents the non-linear friction exerted between the rock mass and its surroundings. Ideally, as the velocity increases the Friction Force F_o initially resists any movement and the cell remains "static". As the force increases it soon reaches a point where the "static friction force" is overcome (W_{max}) and the cell begins to move. As this occurs the friction resistance decreases and the cell's velocity increases.

To successfully model this action the circuit must be able to produce an output in both the positive and negative direction which will initially rise to a set point (W_{max}) before its response decreases towards zero in a non-linear manner.

3.6.1 Non-linear cell block diagram

The block diagram of the non-linear cell is depicted in Fig. 10.

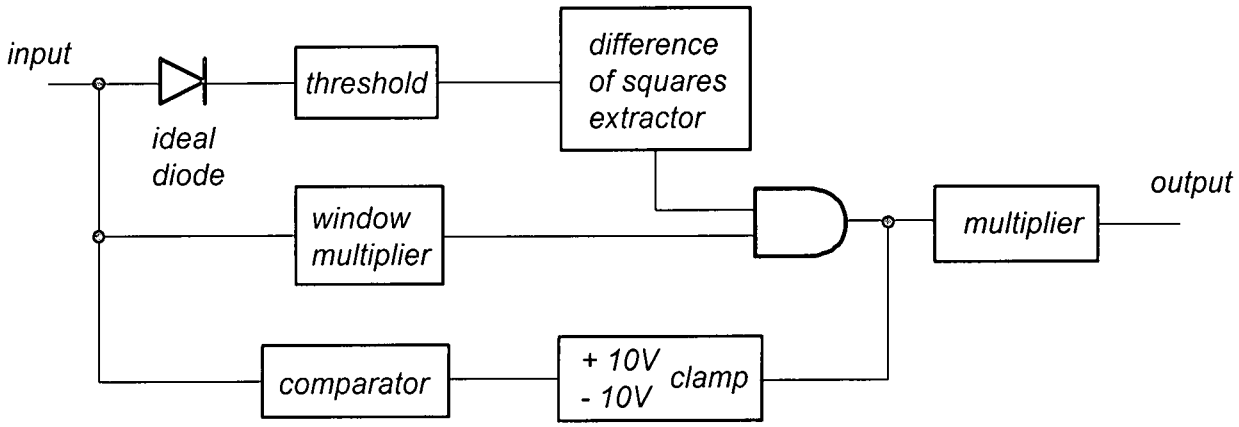

Figure 10

Explanation of the non-linear cell operation

See Appendix #2 (p 55) for a full circuit component diagram of the non-linear cell.

Stage 1 : Ideal diode

The ideal diode rectifies input pulses with no losses [12]. The amplitude of any signal appearing at the input terminal (rising or falling) will appear at the output terminal as a positive signal, with no losses.

The next stage after the ideal diode (IC 1a) is a "buffer" which presents a high impedance to the following stages while incurring no losses to the diode circuit.

The two stages following the buffer are simply amplifiers to provide for gain of the input signal.

Stage 2 : Window comparator

This stage will detect the moment that force is applied. (ie: when a voltage appears at the input). The window comparator introduces a "window" of operation (between +0,6 V and − 0,6 V) where the "force" is allowed to increase before initiating an output response. (The actual level of force is determined by the threshold adjust circuit).

Operation

The two ICs IC 2a and IC 2b both operate as comparators, comparing the input signal against a constant 0,6 V reference provided by diodes D1 and D2. Two complementary circuits are used to cater for both positive or negative input voltage levels.

IC 2c and IC 2d are simply buffers ensuring no loading between the diodes and the comparators. Under no signal conditions the outputs from both comparators should be balanced. This will keep transistor T2 *off* and allow the biasing circuit to keep transistor T3 *on*. Thus holding the input to IC 4d (pin 12) low.

When force is applied (either positive or negative) this will cause the output of either of the comparators to rise, activating transistor T2 which in turn pulls the bias circuit of T3 low enough to turn it *off*. This will allow any signal from the square root extractor (IC 3) to pass through the buffer (IC 4d) and enter the multiplier.

Stage 3 : Threshold circuit

This circuit determines the point at which the applied force will cause movement. Once having reached this point the circuit then exhibits a linear output responds. This linear response is later converted to a non-linear decay by the final stage, the square root extractor.
It has three variable controls:

1. The **maximum force** point.
   This determines the maximum level of force applied to the cell.

2. The **threshold** trigger point.
   This refers to the point at which the residual strain within the rock mass is overcome.
   This sets the point at which the cell will respond to the applied force (ie: the "**shear**" point).
   It controls the acceptable "applied level of force", required to be exceeded before any movement takes place and is set by preset resistor VR1. After reaching this point the "forces" (voltage level) are reduced as movement takes place.

3. The **slope** of response. This refers to the initial decay of the circuit's response.
   Once activated the response of the cell to applied force can be adjusted as to the rate-of-change (or "fall") against the force.
   Slope and ***threshold*** are mutually dependant.

4. Observe output response of IC3 (pin 7 IC3) and vary VR3. This sets the **slope** of the output response.

Stage 4 : Square root extractor

Upon reaching the point of shear force the model is to exhibit a reducing non-linear output response. The output from the threshold/slope stage 3 is linear. This is fed into a circuit which will produce the square root of this value which, in turn, produces the required, reducing non-linear effect.

The square root response produces a non-linear response which is acceptably close enough to an exponential response.

3.6.2 Non-linear cell calibration

The cell is to depict the non-linear friction exerted between the rock mass block and its surroundings as the block's velocity changes. The circuit was created to have variables of:

① Maximum friction force : represented in the model by "W_{max}".

② Friction slip velocity (static friction force) : represented in the model by "Threshold".

③ non-linear force decay : represented in the model by "Slope".

The three variables, shown in the characteristics below, enabled the original response to be varied.

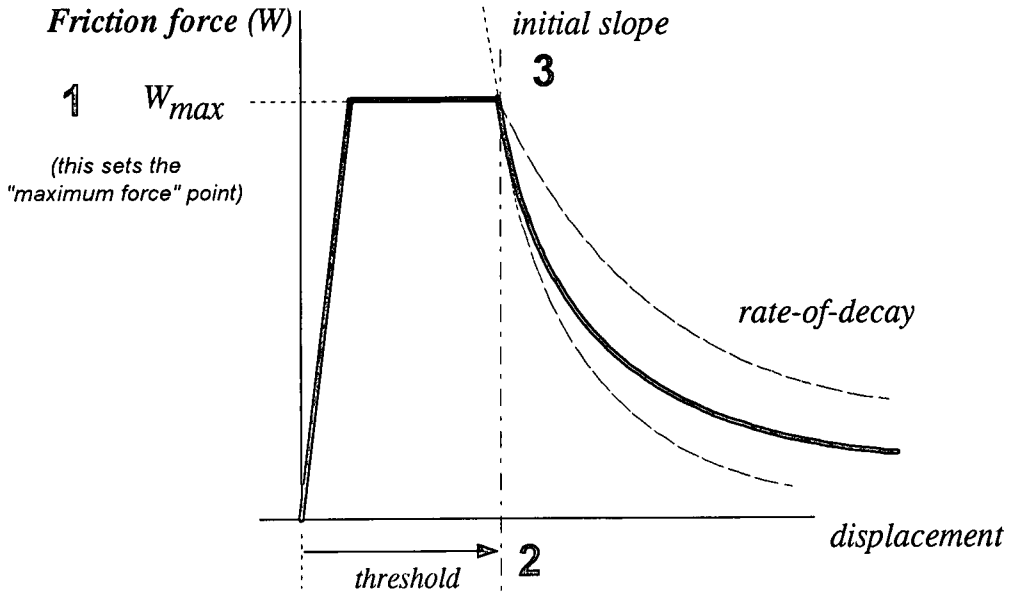

Figure 11

Each variable component was allocated a multi-turn variable potentiometer with which to change its settings. These are found on the top of the non-linear cell circuit-board marked as;

potentiometer 1 : representing the horizontal velocity point *threshold.*

potentiometer 2 : representing the vertical *maximum friction force* point W_{max}

potentiometer 3 : representing the response *slope*, that is the initial decay response.

Because both the slope and threshold settings are mutually dependant (ie: in setting one variable, this would change when adjusting the other), this caused a number of iterations of several adjustments to be perform to finally obtain the desired settings on all three points.

Calibration

The cell was calibrated in the following manner:

1 **Maximum force point**
   i input voltage was set to 1 V (a value above the 0,7 V conduction point of the ideal diode).
   ii output voltage was observed.
   iii trim pot VR_2 was adjusted to set the maximum force point output at a nominal value of 10V.

2 **Threshold point**
   - input voltage was set to a nominal selected value of 6 V.
   - output voltage was observed.
   - trim pot VR_1 was adjusted to set output at 10 V.

3 **Slope**
   - input voltage was set to 10 V.
   - output voltage was observed.
   - trim pot VR_3 was adjusted to set output to the origin point at 0 V.

As an initial test the cell's response was tested under the following conditions:

The maximum friction force point W_{max} was fixed to 10 V while the other two variables were alternately adjusted to obtain the following table of settings.

input (velocity)	output (friction)
0 V	0 V
1 V	10 V
2 V	10 V
4 V	10 V
6 V	10 V
8 V	5 V
10 V	0 V

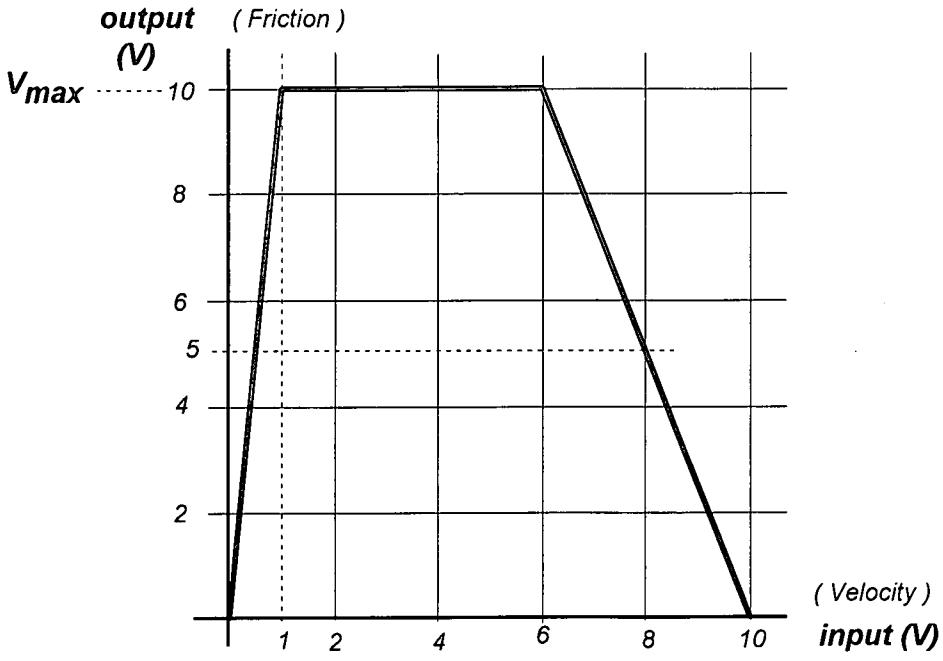

Figure 12

This linear response shows a very good correlation with the expected design.

This output response is now fed via a square root extractor which will produce the square root of this value and hence the required non-linear effect.

3.6.3 Non-linear cell test

As a further test using the same nominally selected maximum friction force W_{max} (10 V) and velocity points as originally calibrated (10V), a comprehensive experiment was performed which yielded the following results:

input (velocity)	output (friction)
1,5 V	9,98 V
2,5 V	9,96 V
3,5 V	9,91 V
4 V	9,5 V
5 V	7,93 V
6 V	6,3 V
7 V	4,7 V
8 V	3,01 V
9 V	1,55 V
10 V	0 V

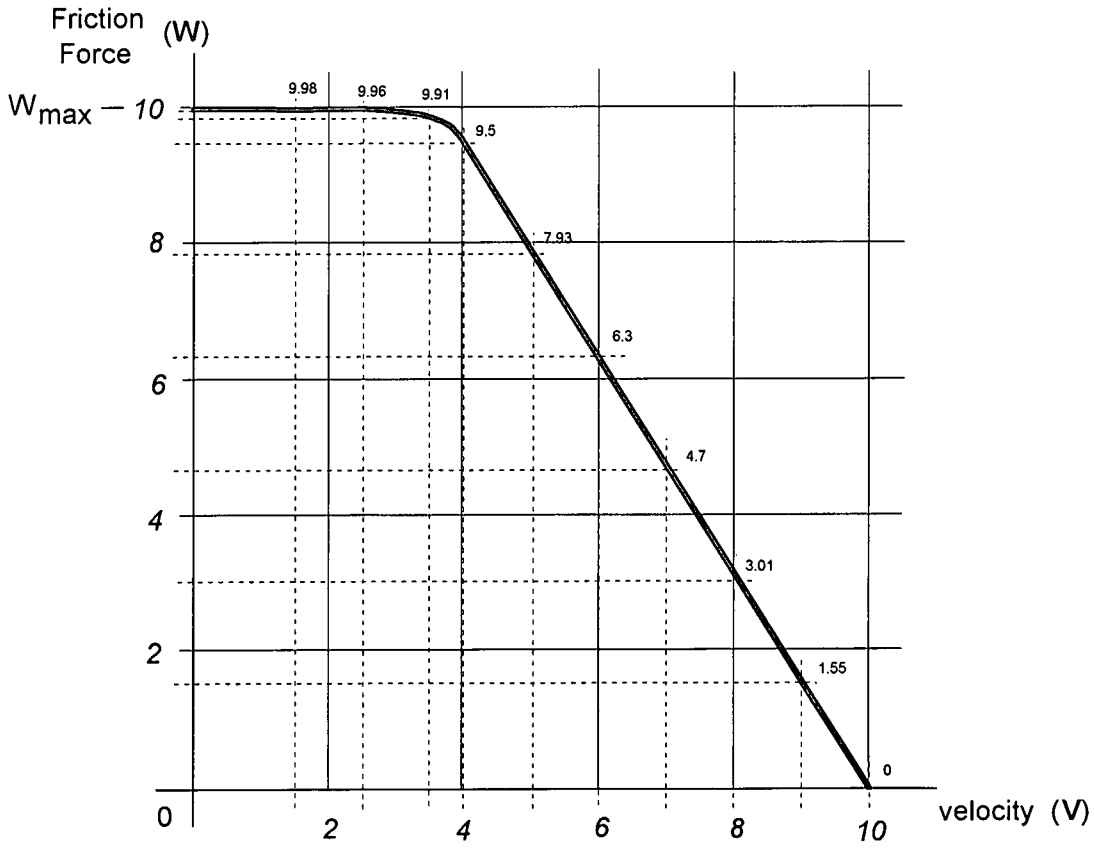

Figure 13

3.7 The master cell

The generalised equation representing motions of all three specific types of rock mass blocks is again given below;

$$m\ddot{x} = k_s^2(x) - k_s^1(x) - k_p(x) + (y)\sin\theta - F$$

Once the non-linear cell was created it required integration into the rest of the analogue computer cell model [15][19], accepting that the non-linear cell is represented by the term (F) in the generalised equation as given above [8].

The equation shows that each term feed into a common "summing" circuit. The various spring stiffness coefficients (*ks*) and lateral leaf spring element coefficients (*kp*) are represented by the previously magnitude scaled terms appearing in the three simplified equations.

After adding each term together using a "summing" circuit the output will represent the *acceleration*. By integrating this output it is possible to obtain the *velocity* and, by a further stage of integration the *displacement* is obtained [23], [25].

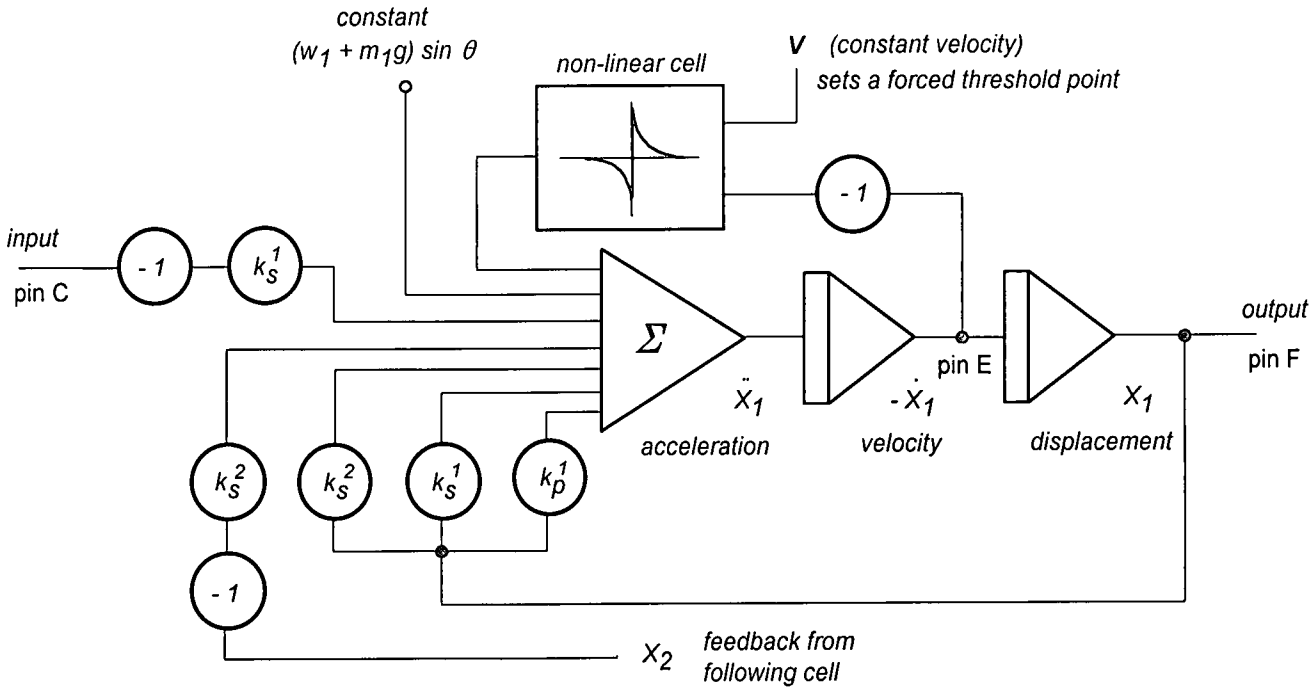

Master Cell Circuit

Figure 14

3.7.1 Explanation of master cell operation

See Appendix #3 (p 56) for a full circuit component diagram of the master cell.

IC #1: U1A, U1B, - incorporates the three internal feedback multiplier circuits.
U1D, U1C - one stage of inversion which also doubles as a buffer stage.
This isolates (buffers) the cell's final output at pin F (ie: the cell's displacement) from the three internal feedback multiplier stages.

IC#2: U2B, U2C - buffer stages
U2A - provides the required gain to the feedback signal from the following circuit stage (arriving at input pin "P").
U2D - provides the required gain to the feed-forward signal from the previous circuit stage, this forms the circuit's primary input (arriving at input pin "C").
U2A and U2D provide both gain and inversion.

IC#3: U3A, U3D - together form the first non-inverting integrator stage.
U3C, U3B - together form the second non-inverting integrator stage.

IC#4: U4A - forms a buffer from reference voltage source.
Also a comparator, allowing preset P8 to set the reference voltage input to the following comparator stage IC#5.
U4B - forms a buffer from reference voltage source.
Also a comparator, allowing preset P7 to set the reference voltage input to the summing stage IC U4C.
U4C - the active stage of the summing circuit.
U4D - inverter (with option of some gain). Brings the output of the non-linear circuit into the correct phase before being introduced to the summing circuit.

IC#5: (LM741) - comparator.

IC#6: - reference voltage. Provides an accurate 10 V reference voltage to ICs U4B and U4B.

The input to the non-linear friction cell for each block is the difference between the block's velocity ($\dot{x}_j$) and the velocity of the moving surface on which it rests. Therefore from eqn. 1-5 (pp. 6) of Bajić [1]; $\phi(x_j - v) = sin \frac{(x_j - v)}{1 + k_f (x_j - v)}$ this shows the movement of each block relative to the already moving surface on which it rests. Coefficient k_f having an effect on the shape of the non-linear cell response.

3.8 Chain of cells

Five cells were constructed with the master cell modified in each case so as to suitably represent each of the three cell types. The cells were coupled as depicted in Fig. 15 in a series fashion with the outputs of each previous cell feeding forward directly into the following cell and becoming one of its input terms, while at the same time each cell's output was fed back to each successive previous cell to also form one of that cell's inputs.

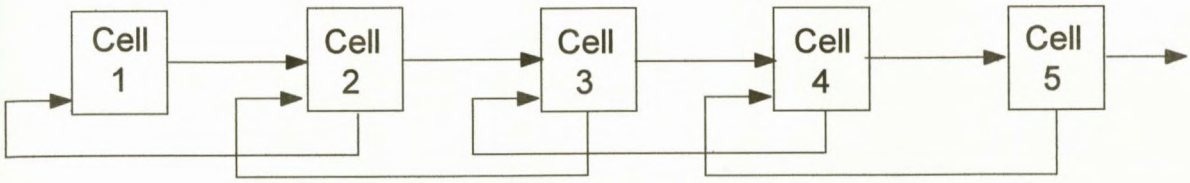

Figure 15

Each analogue circuit was constructed on a single sided circuit board. On the same board, alongside the "master cell" was placed a separate circuit containing the "non-linear cell" with the two sub-circuits being hard wired together.

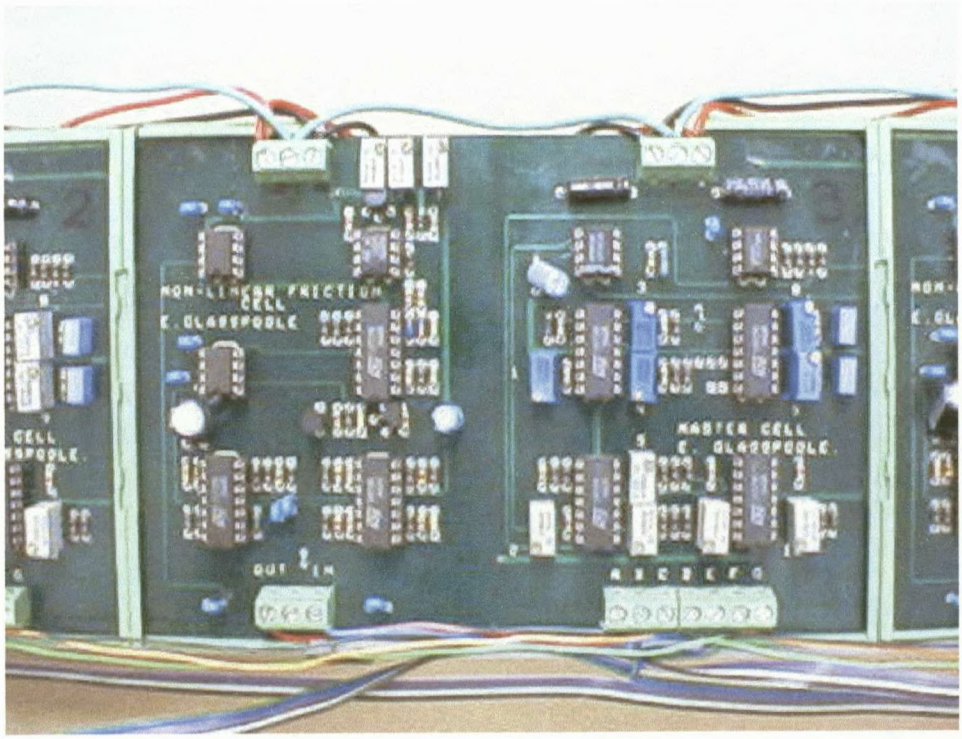

Figure 16 ***A single cell showing the non-linear friction cell to the left and the master cell to the right.***

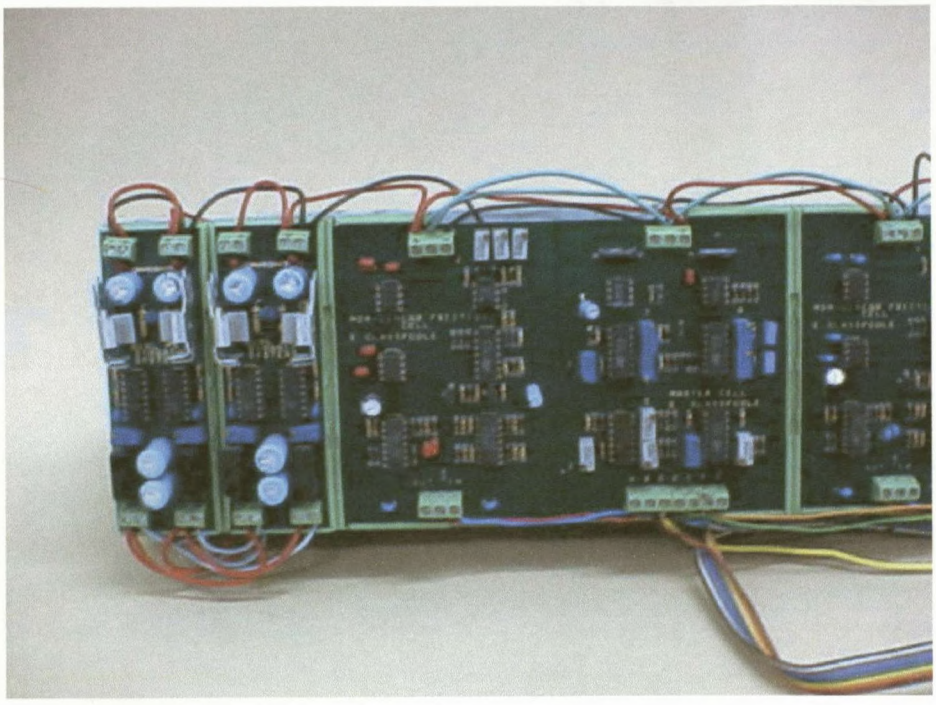

Figure 17 ***Cell number one in the chain together with the regulated voltage supply.***

As the chain contains "*n*" cells, a five cell chain was selected purely for the reasons of size and physical manageability on which to conduct the experiment.

This would incorporate a first cell, an end cell and three intermediate cells. The test chain was rack mounted together with its own stabilised regulated power supply.

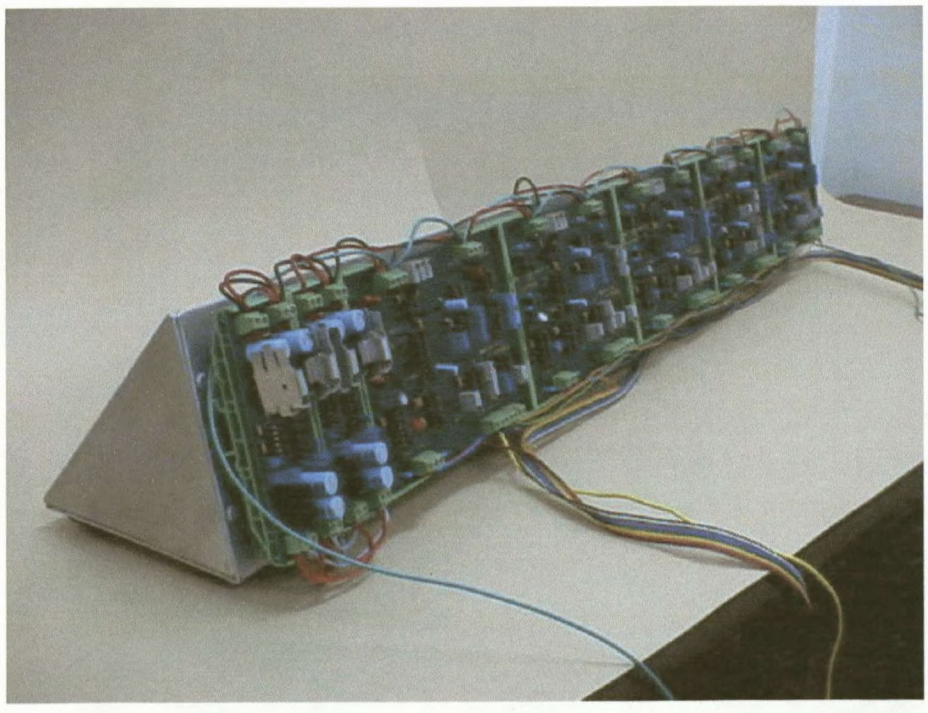

Figure 18 ***Complete test unit showing the chain of five cells.***

3.9 Data acquisition system

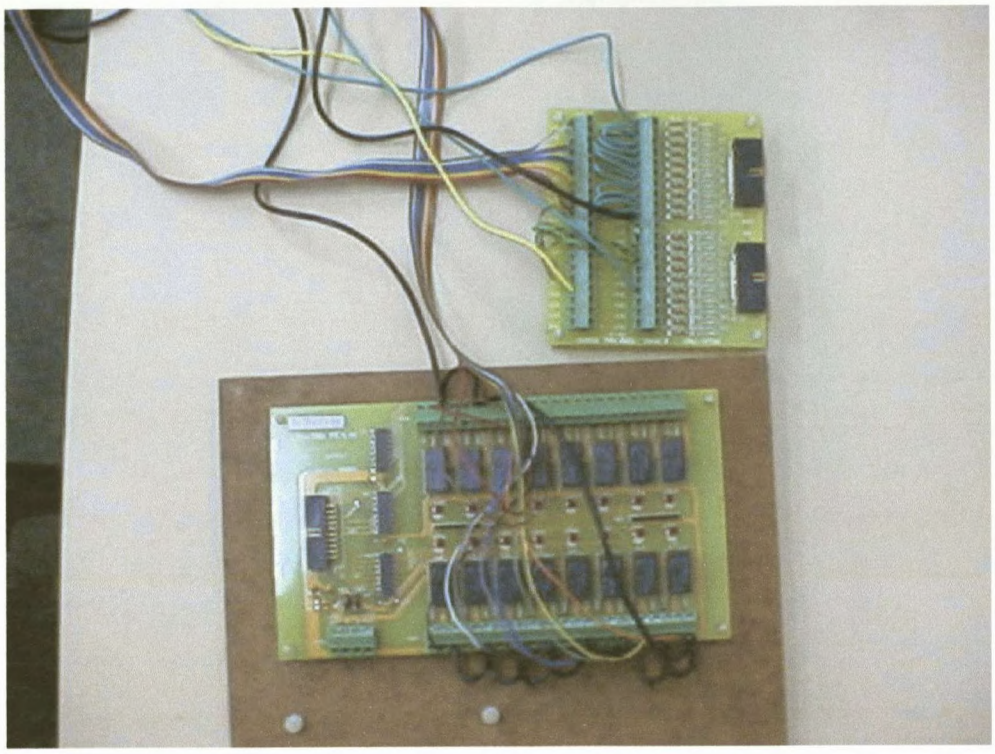

Figure 19 ***Data acquisition interface circuit with digital outputs***
Analogue input interface at the top
Digital output relays at the bottom

The data acquisition system [3] [4] [10] [20] had characteristics that fulfilled the following:

SYSTEM SPECIFICATIONS:

- Sample rate 20/second
- number of channels 10 (16 available)
- storage capability 400 samples/channel (ie: 20 seconds worth of data per channel).
- measuring range ± 10 V
- resolution 1% (12 bits available). This was based on oscilloscope observations that indicated that a 1% resolution was sufficient.
- volt-free contact relays. It was necessary to reset internal timing circuits in the simulator cells at the commencement of a sampling run.

Data for each test run were made available in "flat text" format to enable importing into a spreadsheet programme.
Data acquisition was implemented on a 486 pc using a PC Lab 812 A-D data acquisition card running on TurboPascal 5.1. The software controlled the data acquisition and storage as well as the control of the resetting relays.

See Appendix #4 (p 64) for source code for the A-D converter.

Chapter 4

Experimental Results

4.1.1 Selection and setting of simulation variables

As each cell is designed with a number of variable parameters it becomes a complex procedure to run series after series of tests each with one parameter being adjusted at a time. It was decided to run a series of experiments on the system and observing the results by varying only the three main parameters, while keeping the settings of all other parameters constant. The three variable parameters were:

1. V_{MAX} : corresponding to the maximum force required to achieve slip in the non-linear cell.
2. *Slope* : corresponding to the initial slope of the test surface. $(w_1 + m_1 g)\ Sin\ \theta$
3. *Threshold* : corresponding to a variable external input.

The V_{max} and ***threshold*** parameters are terms which both affect the operation of the non-linear cell and are controlled by adjusting variable trimpots mounted on the non-linear cell circuit-board. The parameters are set within the non-linear cell by adjusting trimpot 2 for V_{MAX} and trimpot 1 for the *Threshold*.

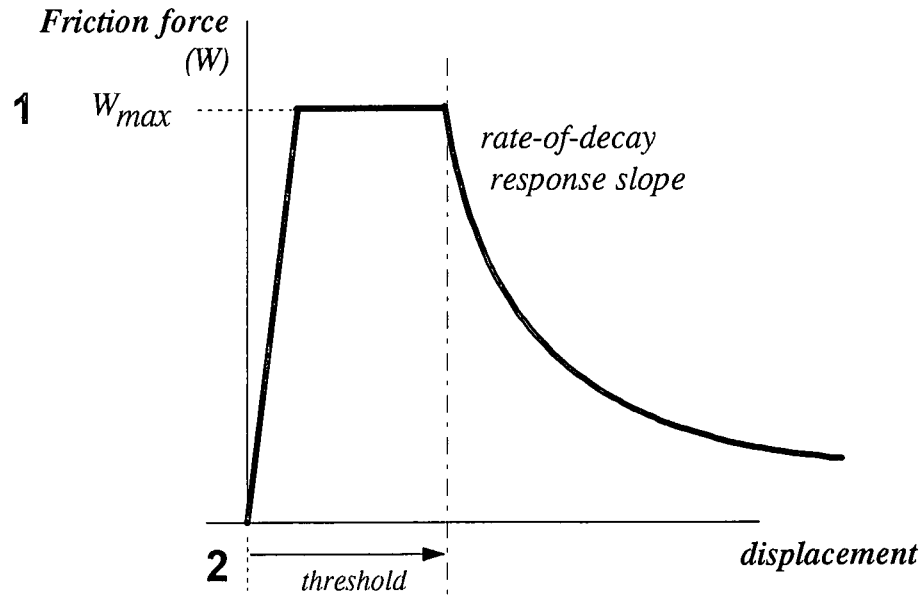

Figure 20

The ***slope*** parameter is controlled by an external dc offset voltage representing the constant term $(w_1 + m_1 g)\ sin\ \theta$ and is applied to the master-cell circuit via an external input, as shown in the master-cell circuit below.

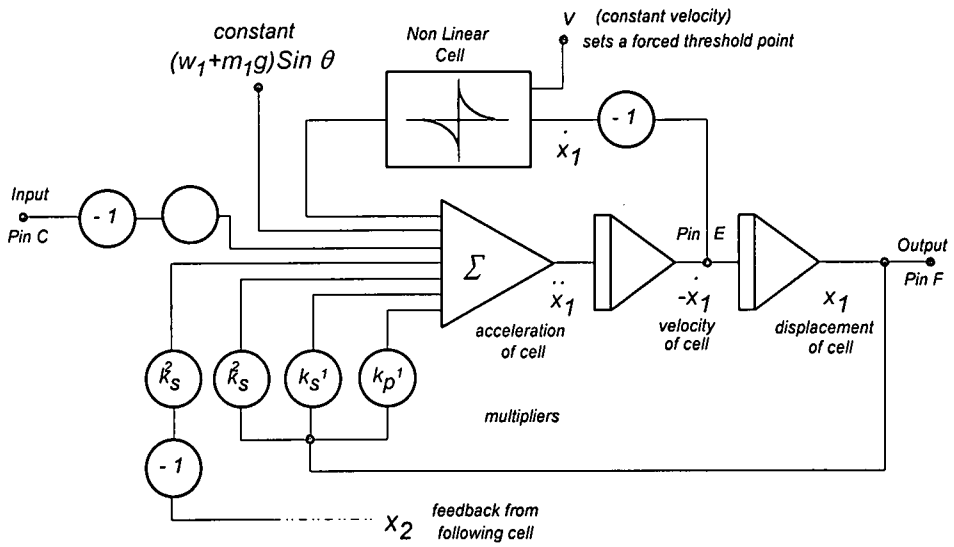

Figure 21

A series of tests were run. With three variable parameters this lead to the development of a matrix table of results, allowing each set of data to be translated into its own graph describing the model's operation.

Rather than present a complex array of tables of values it was decided to present three representative graphs from the table of results. They represent the test circuit's response in three different scenarios which produced the most significant results and which were each tested under the following variable settings:

	Test 1	Test 2	Test 3
V_{MAX}	4,5 V	7 V	10 V
Slope	8 V	6 V	0,5 V
Threshold	0,5 V	6 V	8 V

4.1.2 Simulation parameters

The simulation parameters were kept constant during each test. It was important to keep within the limits of circuit supply voltages so as not to drive the system into saturation conditions. All other variables were kept constant during the tests.

4.2 Simulation results

4.2.1 Type I test

Aim

By introducing a high damping coefficient while simultaneously simulating a small slope, the test conditions are so chosen as to contribute to a rapidly decaying response from the chain of cells. It is intended to show that the model will simulate a controlled, damped response. In terms of seismic events this would correspond to a short, quickly disappearing earthquake.

Test conditions

i Slope simulation *Sin* θ, which represents the angle upon which the five cell chain model rests is reduced to a very small angle to simulate a near horizontal fault plane.

The electrical equivalent in the model are : $sin\ \theta = 0{,}5$ V.

ii the two variable responses of the non-linear cell were both set at an initially high value to simulate high levels of friction.

The electrical equivalents in the model are : $V_{max} = 10$ V

Threshold = 8 V

Experiment Description

Initially it is assumed that the system is in equilibrium. As there is zero response from any of the cells they correctly model inert rock masses which lie at their reference positions with an initial displacement of zero. Hence their velocitys are also zero and so, leading from this they each release zero energy.

Initial excitation of the system is provided by means of a controlled, externally applied emf to simulate an impulse caused by sudden movement of the rock mass layer.

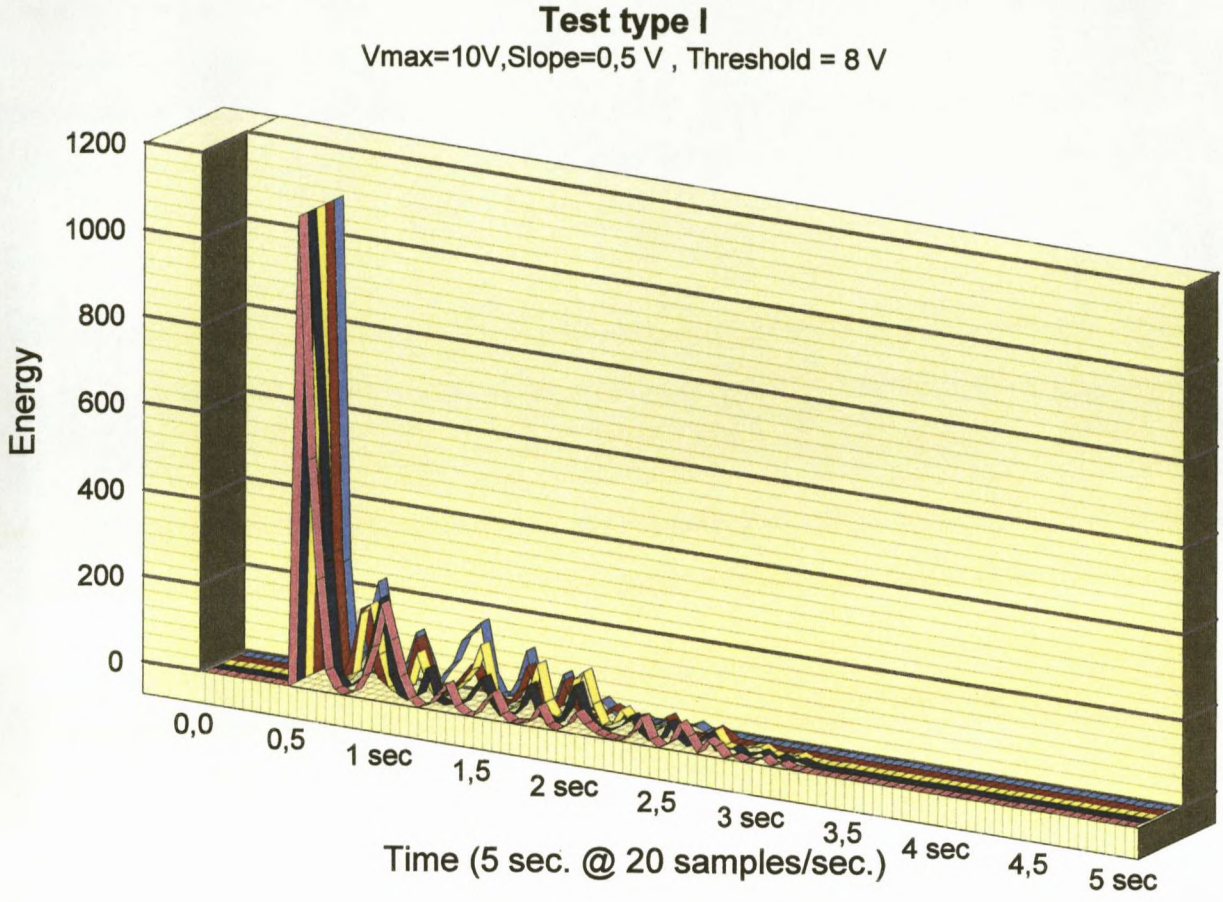

Figure 22

Comment

Upon receiving the initial activating impulse, the five cells begin to respond in an irregular manner, with low releases of energy from various cells.

It is observed that the duration of this low level "random" energy release is for a period of approximately two and a half seconds, after which the responses of all five cells fall away to zero. With no further releases of energy during the test period this indicates that the cells in the system have each reached their new equilibrium positions and that the system is once again in a state of equilibrium.

This test effectively models a situation in which the behaviour of the test cells represents a damped seismic response [24].

4.2.2 Type II test

Aim

By decreasing the values of both the friction damping coefficients and increasing the slope of the lower surface it is hoped that the circuit conditions are set to promote a more unstable response. This would correspond to an initial seismic shock with prolonged seismic activity that dies after some time.

Test conditions

i Slope simulation $sin\ \theta$ which represents the angle upon which the five cell chain model rests is increased.

The electrical equivalent in the model are: $sin\ \theta = 6$ V.

ii the two variable responses of the non-linear cell were both reduced to simulate decreased levels of friction.

The electrical equivalents in the model are: $V_{max} = 7$ V

Threshold $= 6$ V

Experiment Description

As with the Type I test it is initially assumed that the system is in equilibrium.

Initial excitation of the system is provided by means of a controlled, externally applied emf to simulate an impulse caused by sudden movement of the rock mass layer. The magnitude of the applied stimulus is the same as in Test I.

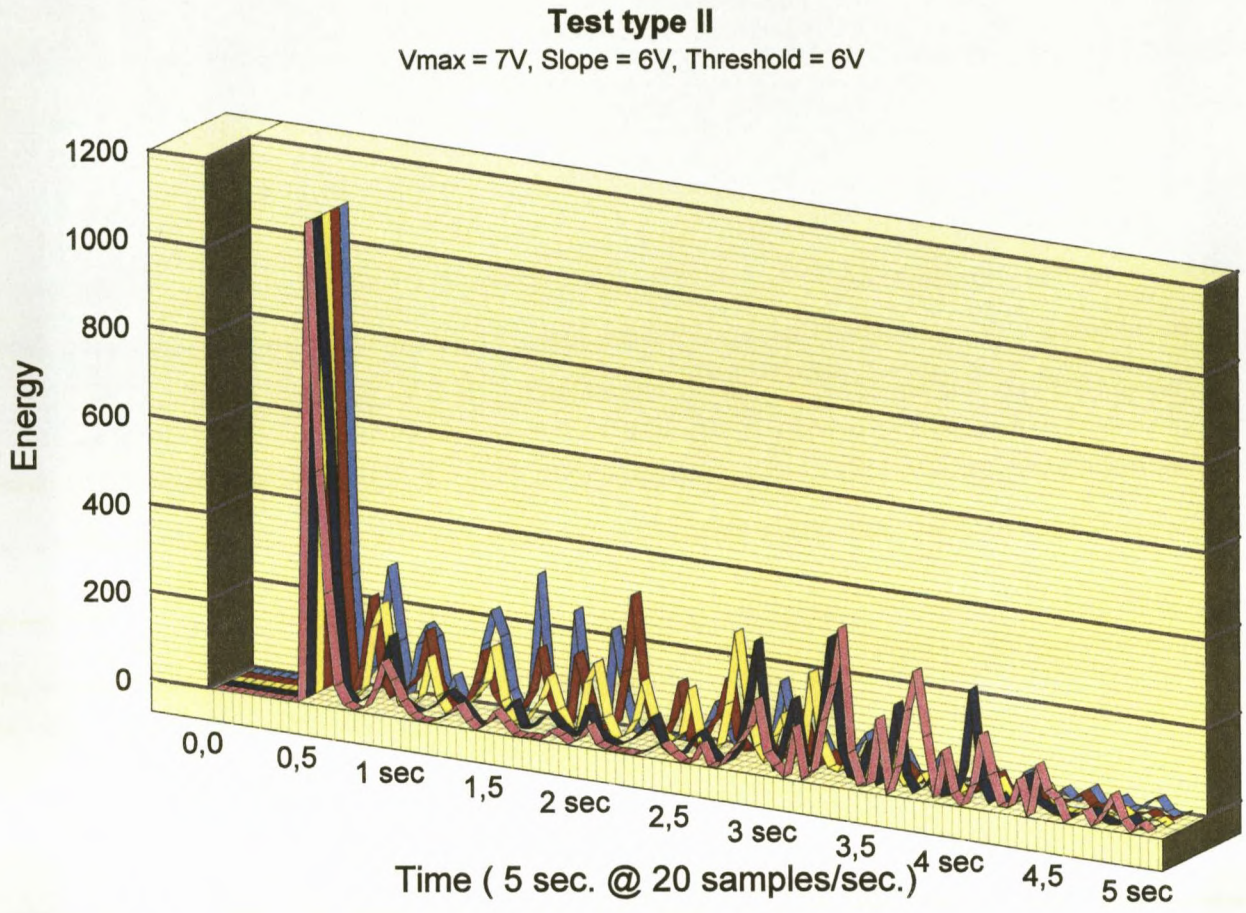

Figure 23

Comment

Upon receiving the initial activating impulse, the five cells begin to respond irregularly, with low releases of energy from each of the cells. The overall conditions of the system, imply a prolonged energy release for several seconds after which the system appeared to be settling and becoming more stable. At no point during the test period did any of the cells display any tendency to simulate release of large quantities of energy.

From the graph it is evident that the first cell initially releases a high level of energy which, on closer inspection, appears to be carried in a wave motion to each succeeding cell resembling a "chain" reaction. However after about four seconds this phenomenon soon dies away and the entire system displays a tendency to revert to a more stable state.

4.2.3 Type III test (The Underdamped "chaotic" situation)

Aim

The values of both the friction damping coefficients are further decreased while the slope of the lower surface is further increased. Under these conditions it is hoped that the conditions within the test chain are created so as to yield a "violent" chaotic behaviour of the system if possible. The prime aim of the test is to see if such a condition can be created, similar in type to that created by the digital model of Bajić. (See: Type 1 Experiments. Page 18). In a realistic situation this will correspond to a seismic event with aftershock events. The initial, relatively small seismic shock, is amplified in time due to the conditions in the rock mass.

Test conditions

i Slope simulation $sin\ \theta$ which represents the angle θ upon which the five cell chain model rests is increased.

The electrical equivalent in the model are; $sin\ \theta = 8$ V.

ii the two variable responses of the non-linear cell were both further decreased to simulate even lower levels of friction.

The electrical equivalents in the model are: $V_{max} = 4{,}5$ V

Threshold $= 0{,}5$ V

1. As the potential representing the slope is large this represents a test in which the chain of blocks under test is resting upon a large sloped incline.

2. Also as the threshold voltage is reduced this will contribute very little to the damping of each cell's response.

3. The maximum force necessary to be exceeded before the non-linear cell responded was also reduced to stimulate a more rapid non-linear behaviour of the model.

Experiment Description

Initially it is assumed that the system is in equilibrium.

Initial excitation of the system is provided by means of a controlled, externally applied emf to simulate an impulse caused by sudden movement of the rock mass layer.

Results

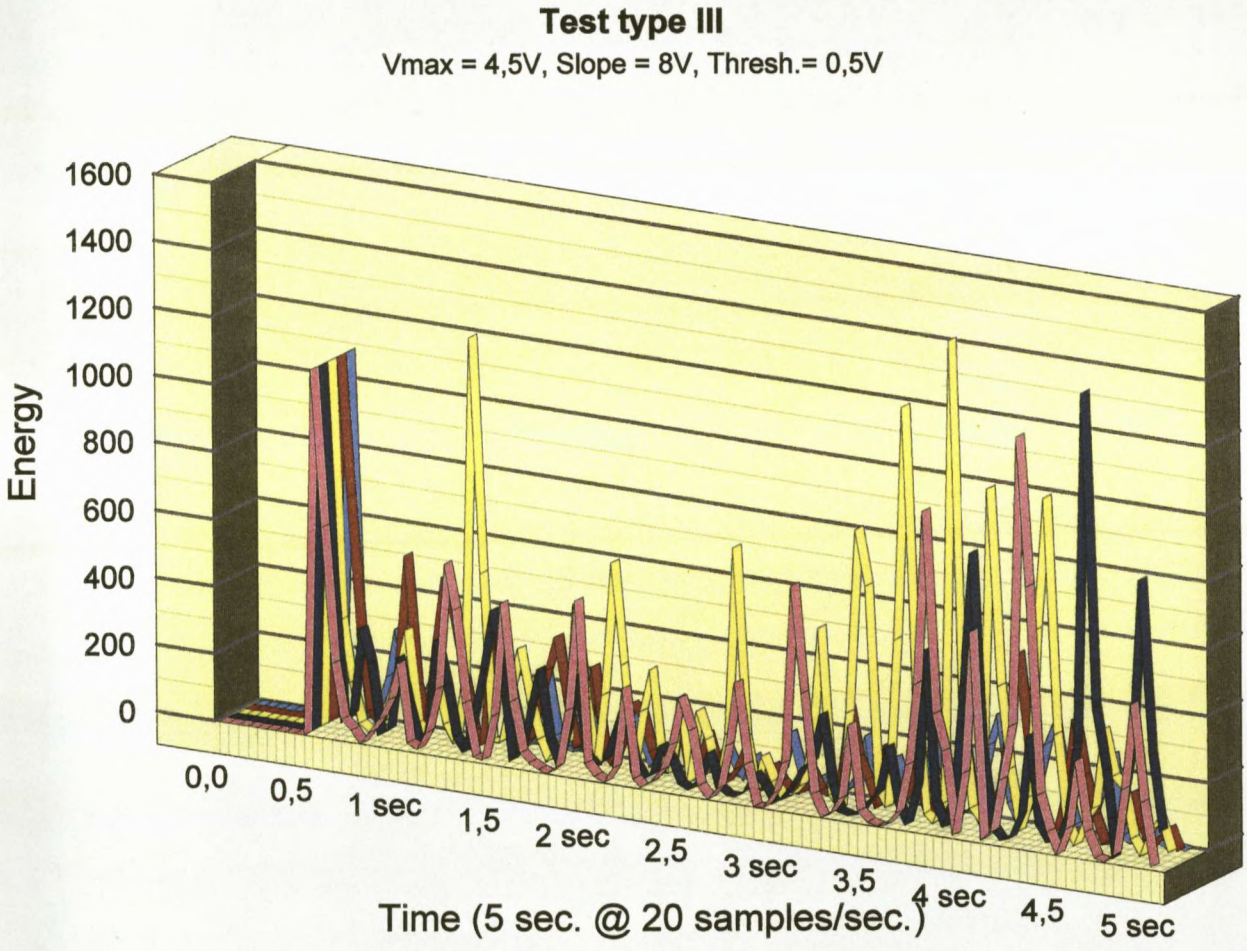

Figure 24

Comment

Upon receiving the activating impulse, the five cells each begin to respond in a random manner, with sporadic high releases of energy from various cells. However after two to two-and-a-half seconds these energy releases from most of the cells appear to dissipate and the system gives the impression that it is heading towards a more settled, damped state. This is possibly because these cells are transferring their energy to other cells, which later transfer it back to re-energise the blocks.

Soon after this, beginning at three seconds, there appear large releases of energy from many of the cells, each far exceeding the initial activating energy impulse, also indicating an increase in the rock mass block's velocities. When summed the total energy released by the system appears to rise dramatically. This transferred energy appears to be stored in the third cell which displays increasing energy levels while those of the other cells are declining. After approximately three seconds it appears that this "stored" energy in cell three may be the catalyst for triggering the release of energy "stored" within the other cells. This appears in the rapid rise of energy release in most of the other cells. Nearing the end of the test period it appears as if the energy release is once again beginning to subside.

However it should be noticed that the additional (excess) energy of the blocks appear to be the consequence of the potential energy contained in the rock mass environment of the moving layer. Hence the model used qualitatively correctly describes this phenomenon.

This test clearly demonstrates the development of a chaotic system. The results are qualitatively similar to those achieved in the Type 1 experiments of [1], with the following comments;

1. The initial damping could be attributed to the torsion element coefficient k_p which couples each block to the stationary surface.
2. The constant $sin\ \theta$ representing the angle of the surface on which the block rests is also quite large in this test condition.
3. Upon close study of the five individual results it can also be seen that the model's response bears close similarity with the one-dimensional wave equation.
4. This model clearly shows that it is capable of producing a "violent" chaotic behaviour similar to the Type 1 experiments of [1].
5. The more disturbed mass appears to be the last of the five blocks showing early and continuous large releases of energy while the centre (or third) block shows a large early release of energy greater than the initially applied impulse. This centre cell continues to exhibit more violent behaviour which might be the main contributing factor towards the chaotic behaviour of the other cells after three seconds into the experiment.
6. The results also show an increased level of energy, greater than that initially used to stimulate the chain. This could indicate the beginnings of a more violent release of energy, possibly leading toward an earthquake situation.

The selection of scale factor and supply voltage limitations could possibly be a leading consideration contributing to errors.

The results obtained from the test analogue circuit comply closely in response with those obtained by Bajić [1]. In comparison with his results it is evident that there is a marked improvement in the response time of the analogue simulation circuit. The response time is also clearly not affected by the number of cells used in the chain.

4.3 Analysis of displacements of two adjacent rock masses

Analysis

From the results of the Type III test, two adjacent rock masses (modelled by cells 2 and 3) were selected to perform a comparative study of their respective displacements. Such a study can reveal much about the developing conditions which exist within the rock mass layer during a developing chaotic situation.

↕D ↕E

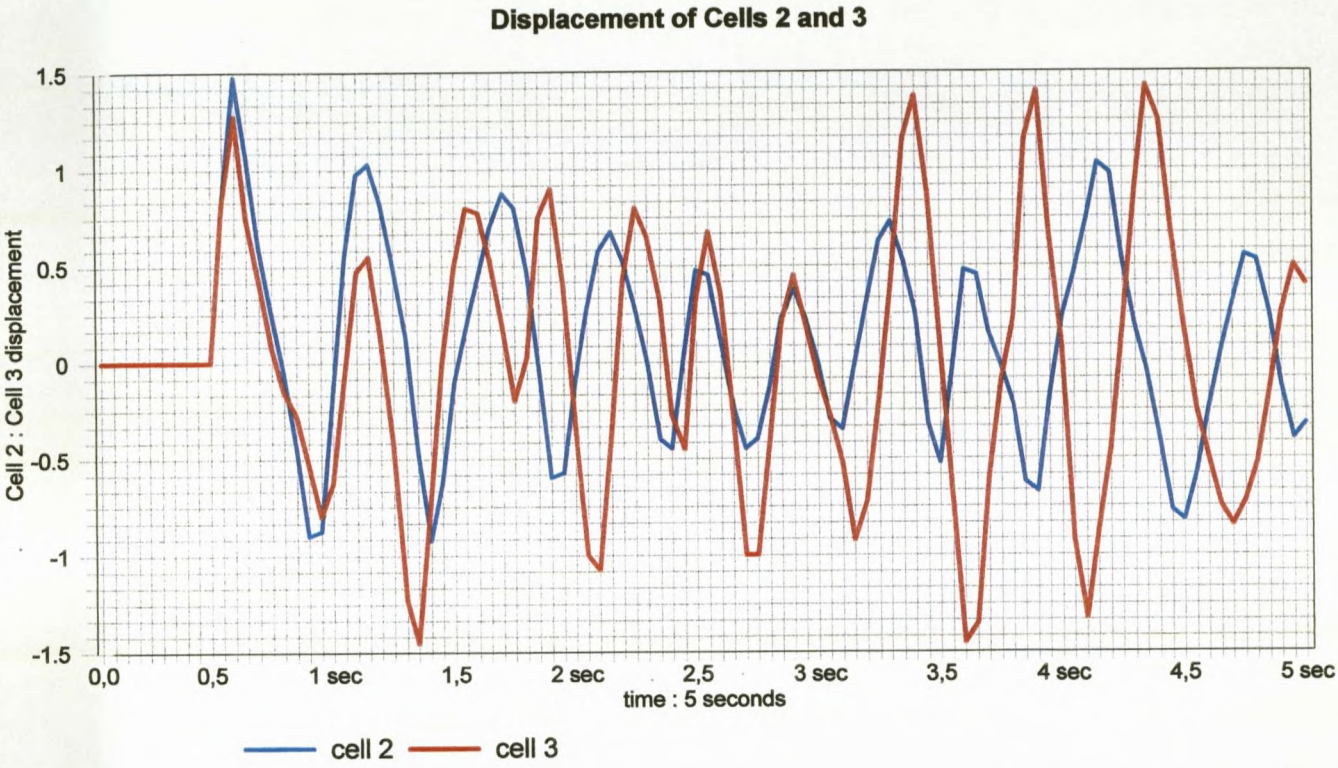

Figure 25

↕A ↕B ↕C

Upon studying the displacement of both masses the following is evident:

1. At points during the test period the two masses experience both compressive and tensile stresses. Point A clearly shows a *compressive stress* point where the displacement of cell 2 is positive while that of cell 3 is negative, indicating that the cells are "moving together". At this point large energy could be released causing surface disturbance at the point at which the moving wave will have reached at this time. This effect again appears at point D and point E. Also, effects of behaviour indicated by points A, D, E can lead to material breakdown.
   Point B and point C show the opposite effect of *tensile stress* where the displacement of cell 2 is negative and that of cell 3 is positive indicating that the cells are "moving apart" from each other. It is at this point that that particular mass is placed under severe tensile stress which, if increased could rupture, depending on the elastic limits of the material.

2. It is also clear that both waves exhibit a cyclic pattern which conforms in principle to that of a primary longitudinal P-wave. The frequency of the waves can be found by recording the period of each cycle. This is estimated to be approximately 0.5 second. Hence knowing that frequency is the inverse of period:

T = 0.5 s then frequency $f = \frac{1}{T}$

$$= \frac{1}{0.5}$$

$$f = 2 \text{ hertz}$$

3. Between Point A and Point D the regular "cyclic" pattern appears to decay in amplitude but, at Point D this amplitude suddenly rises indicating large increases in rock displacement. Again, depending on the rock mass elasticity and composition this could be indicating the development of severe material ruptures.

4. At times during the test period both rock masses display common displacements where their displacements are both in the same direction, at the same moment in time. Between Point A and Point B this is most evident.

4.4 Analysis of energy release within the test chain

Energy density

Probably the single most important feature of any wave is the energy associated with the motion of the medium as the wave passes through it. Usually we are not concerned with the total energy of the wave but rather with the energy in the vicinity of the point where we observe it(the *energy density*).

In the rock mass there is both a *kinetic energy* which is measured per unit volume, as well as a *potential energy*. As the medium oscillates back and forth, the energy is converted back and forth from kinetic to potential form, the total energy remaining fixed (assuming an undamped medium). When a particle is at zero displacement, the potential energy is zero and the kinetic energy is a maximum, and when the particle is at its extreme displacement the energy is all potential.

We are also interested in the rate of flow of energy and we define the intensity as the quantity of energy which flows through a unit area normal to the direction of wave propagation in unit time.

The general expression for energy is: $E = \frac{1}{2} m v^2$ Joules

where: v is the velocity of a body,
m is the mass of the body.

This expression is used to describe the energy released within the system during the test, with the initial energy released upon application of initial stimulating impulse being $E_o = \frac{1}{2} m v_o^2$, and the energy released at the i - th time interval during the test is $E_i = \frac{1}{2} m v_i^2$.

Where:

E_o is initial energy introduced to the system upon trigger impulse. At time t = 0 seconds.

E_i is energy released at successive time intervals during the test.
At times t = (0 sec.+ 50 ms), ... 5 sec.

v_o is initial velocity of each cell.

v_i is velocity of each cell at successive time intervals during the test.
At times t = (0 sec.+ 50 ms), ... 5 sec.

m is 10^{10} kg (values as used in [1]).

By summing the energy present at each test moment during the test period and comparing each sample with the initial amount of energy applied (E_o) it is possible to deduce the comparative ratio of simulated energy release during the test. This energy originating from the accumulated energy within the system as a result of the initial conditions created by the rock mass being supported at rest upon a slope against friction and gravity.

Total energy E_{tot} released across test period, from 0 sec. to 5 sec. is $E_{tot.} = \sum_{v=1}^{n} E_i$

Relative increase in released energy related to $E_o = \frac{E_{tot.}}{E_o}$

The test results of the Type III test were analysed to reveal energy released by the system during its developing chaotic condition.

1. The graph shows the relative increase in total energy released in the first rock mass of the test chain during the period of the test. It shows the energy released in the rock mass relative to the initial trigger impulse energy and that, by the end of the test period this test mass had already released a relative energy level equal to just over six times the initial energy of the triggering pulse.

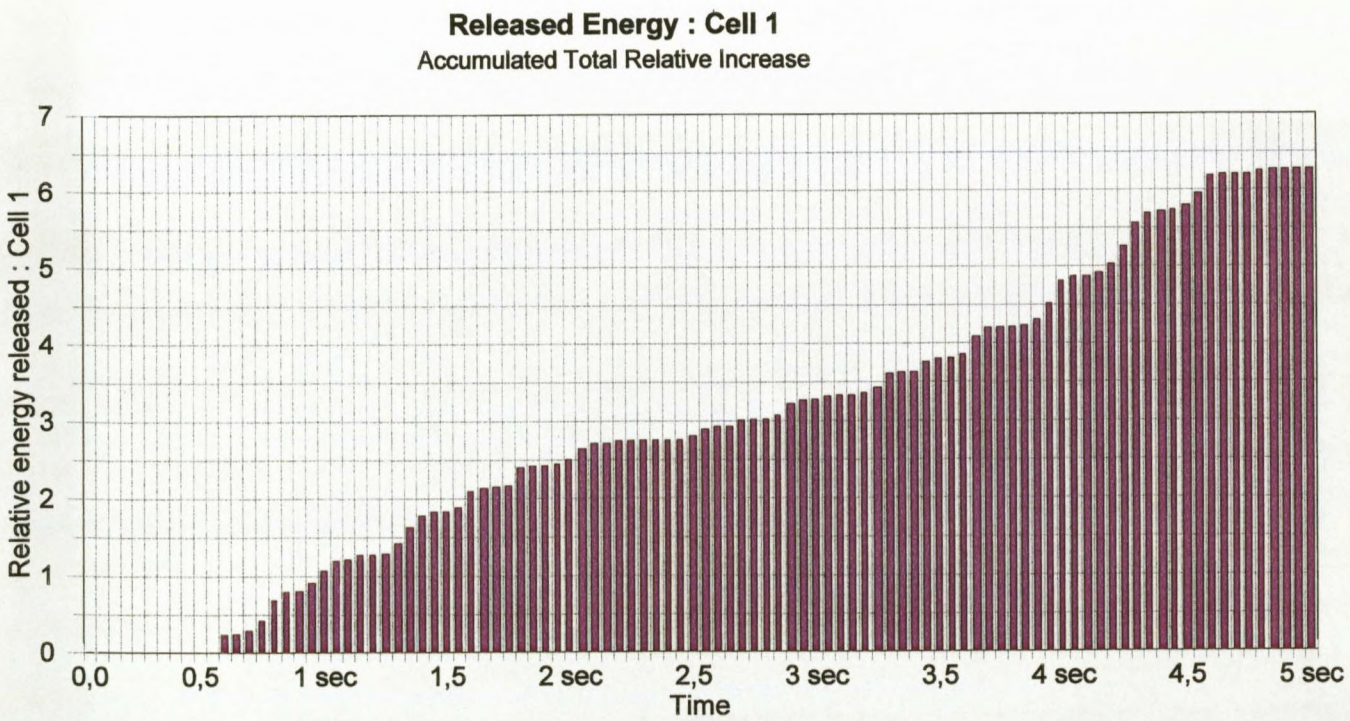

Figure 26

2. This graph shows a comparative release of energy in each of the five rock masses of the test chain. The energy released in cell 3 being the largest at just on eighteen times larger than the initial energy input pulse.

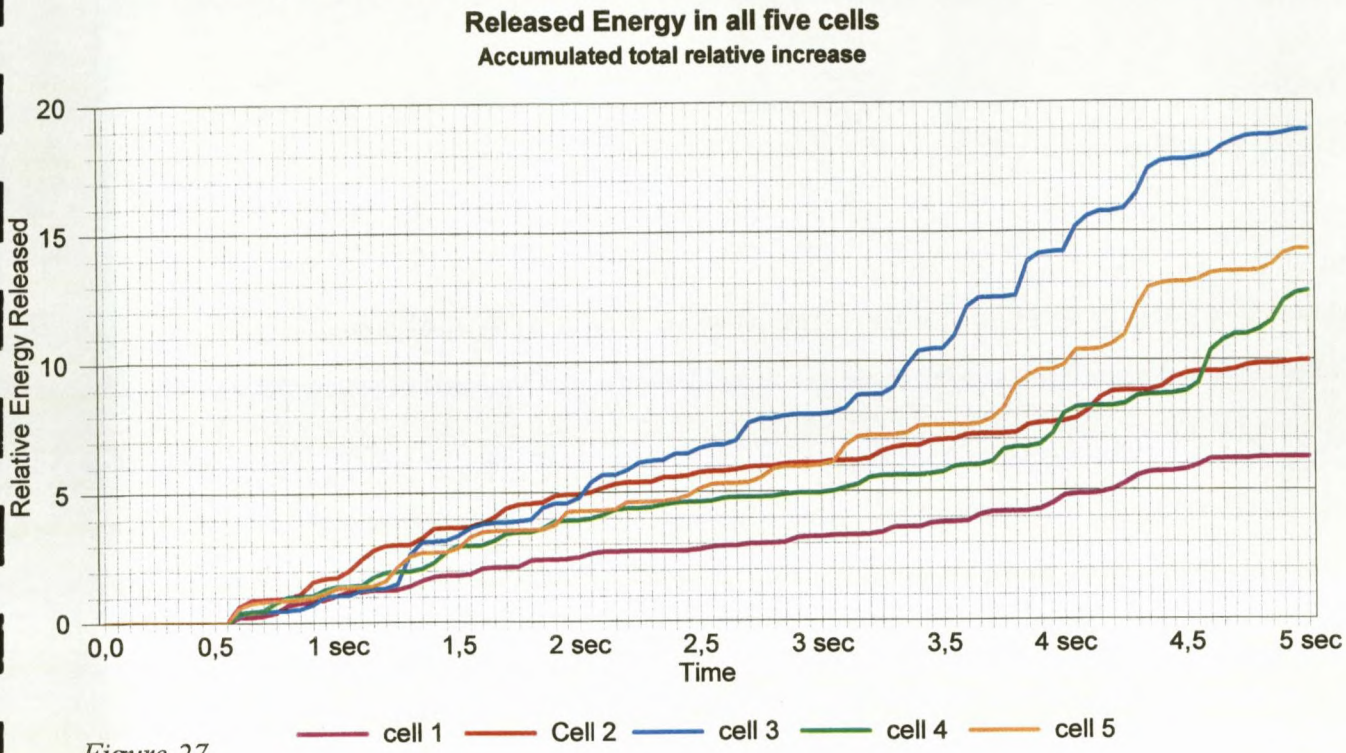

Figure 27

3. This graph shows the combined energy released by all five rock masses in the test chain across the test period. It indicates that the total energy released by the entire test chain is just over sixty times that of the initial energy of the triggering pulse.

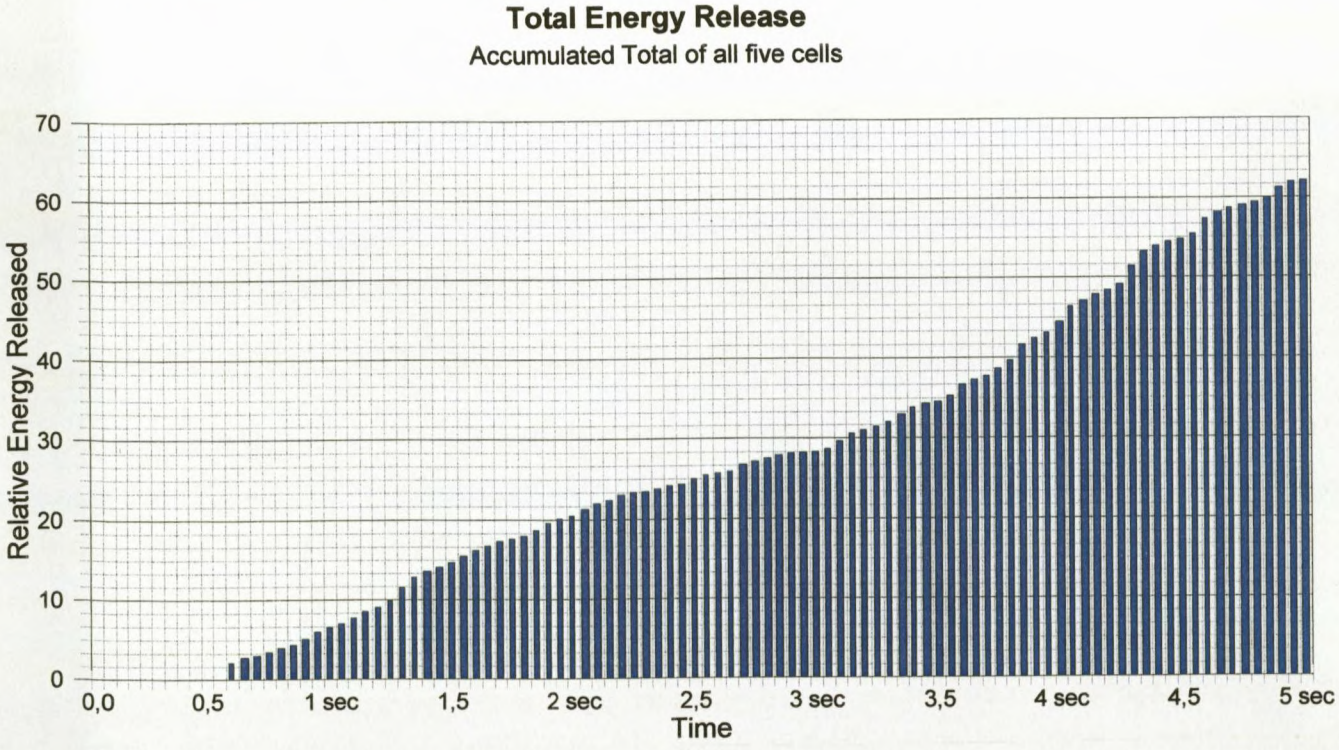

Figure 28

Chapter 5
CONCLUSIONS

The aim of the research project was to develop an analogue simulation network model and an associated data acquisition system for the simulation of particular dynamic phenomena in rock mass, that would produce simulation times less sensitive to the change of the order of the model, compared with the simulation achieved via a digital computer. The model was to describe the dynamical behaviour of a part of the rock mass and it was to completely emphasise these effects, while neglecting other phenomena occurring during the event. With the results produced it is clear that the main aim of the project was achieved. The model produced qualitatively similar results to those achieved in [1] in a series of experiments.

The model clearly demonstrates that it describes the dynamical behaviour of a part of the rock mass it is intended to simulate. It shows the elastic properties of the material by way of the stiffness coefficients of the springs in the model k_s and k_p. The events simulated in these experiments were intended to represent the sudden weakening of a plane in a rock mass (similar to the situation when new fractures appear in the rock mass). The model then demonstrates the results of such a weakness on the dynamics of the rock mass. The model shows how under certain conditions an initial impulse of energy is able to spread through the system and provoke disturbing, chaotic uncontrolled events.

The results produced by Test type III displayed an increasing level of "random" release of energy, which relates directly to a greater chance of rock deformation. As demonstrated this is due to simultaneous, different either positive or negative velocities of each rock mass block (ie: the rock mass either moves forward or backward). At times of opposite velocities this resulted in neighbouring rock masses colliding, leading to an increase in pressure between the masses, resulting in a splitting of the rocks and a release of energy in a direction different to that of the rock movement. It is this event which can be shown to lead to the tendency for the occurrence of a chaotic event.

Criticism of the model

A problem which was evident in the experiments was the difficulty in relating correctly the values of model parameters with the real physical values they each represented. Given these obstacles this analogue model could serve mainly as a subsidiary tool for the analysis of dynamic phenomena of a rock mass, which is more of a qualitative than a quantitative nature.

Limitations of the model

Energy is transmitted in three ways. Radiation losses, convection and internal damping. This model does not take the first (radiation) or the second (convection) manners into account. It places most emphasis on the third manner (internal damping) which is represented by spring coefficients.

This 1-D five cell model is faced with rigid boundaries (constraints) by being a limited, single dimensional linear model and hence it is incomplete and not a true representation of reality. This model is adiabatic (energy cannot escape) therefore within these limited constraints any simulated energy release by the model cannot escape and hence, it will build up. This does not occur in the "real world" as, in the real case there also exists the other two methods of energy transmission, radiation losses and damping losses, which allow the energy to escape in the form of a wave.

In this model the inertial masses are lumped together with no strains existing within each mass, i.e. they are rigid. In the opening remarks of his work, while describing the terms used to develop the mathematic model, Bajić comments that "*coefficients k_s and k_p roughly represent the elastic properties of the contact region*". Coefficients k_s and k_p are held to be linear (which is implicit in the original equations). This is not a true life representation but, assuming that with the passage of P-waves the displacements are small, both coefficients k_s and k_p may be considered as constant, ie: Hooke's Law applies.

Because the system is linear (implied in the differential equations) the system's boundaries are rigid therefore all energy generated within the test cells cannot be radiated away. Hence energy will decrease only in the internal elements. This model will perform better if it could be constructed to mimic stress waves, ie: have a successive infinite array which will radiate energy away.

Pointing to further work

The model used here represents a 1-D stratum of a multi-dimensional system. It therefore invites an investigation of a multi-dimensional model. As a chain reaction effect was demonstrated by the relative motions of the rock masses this indicates that more sophisticated experiments could also produce some other effects, for example chaotic system response under the appropriate conditions. Also as this is a simple 1-dimensional model, the creation of more sophisticated 2-D and even 3-D models could reveal more insight into the behaviour of rock mass layers as they would allow the correct dissipation of energy. Thus with a more complex model with the output from one layer acting as the input to the next layer, 2-D or 3-D events can be simulated. This multi-level array model would cater for more "real world" energy transmission via stress waves (shock waves).

This model could prove a useful starting point for further investigation into analogue, real time simulation of underground activity. It could be useful for qualitative investigation in seismology because of its simplicity as well as the large number of effects that it can exhibit. The nature of the analogue circuit also makes it inherently relatively fast acting.

Chapter 6

References

1. Bajić V. (1992), *Possibilities for the Utilization of a Mechanical Model of Dynamic Rock Mass Behaviour* (a pilot study), Chamber of Mines Research Organization, RSA.

2. Burridge R. & Knopoff, L. (1967), *Model and Theoretical Seismicity*, Bull. Seismol. Soc. Am., (pp.341 - 371).

3. Bissell, C.C. (1994). *Control Engineering*, Chadman & Hall, London. (pp. 171 - 187)

4. Bolton W. (1992), *Control Engineering*, Longman Scientific & Technical, England. (pp. 288 - 289)

5. Boylestad R.L. and Nashelsky L. (1999), *Electronic Devices and Circuit Theory*, Prentice Hall International, New Jersey. (pp. 622 / 666 - 667).

6. Brady B.H.G. and Brown E.T. (1985), *Rock Mechanics for Underground Mining*, George Annen & Unwin, London. (pp. 86 - 124).

7. Carlson, J.M. & Langer, J.S. (1989), *Mechanical Model of an Earthquake Fault*, Physical Review A, (Vol.40, No.1, pp 6470 - 6484) .

8. D'Azzo J.J. (1995), *Linear control System Analysis and Design*, 4 th. Edition, McGraw-Hill, New York. (pp. 144 - 145)

9. Domingues, J. & Alarcon, E. (1981), *Elastodynamics*, Chapter 7 of *Progress in Boundary Element Method* - Vol.1 (C.A. Brebbia, Ed.), Pentech Press.

10. Franco S. (1998), *Design with Operational Amplifiers and Analog Integrated Circuits*, 2 nd. Edition, McGraw-Hill International, Boston. (pp. 116 / 564 - 570).

11. Hoek E. and Bray J.W. (1992), *Rock Slope Engineering*, 3 rd. Edition, Institute of Mining and Metallurgy. (pp. 22) (pp. 24 - 29)

12. Jacob J.M. (1993), *Applications and Design with Analog Integrated Circuits*, 2 nd Edition, Prentice Hall International, New Jersey. (pp. 504 - 505) (pp. 507 - 508).

13. Jager J.C. & Starfield, A.M. (1974). *An Introduction to applied Mathematics*, University Press, Oxford.

14. King, C.Y.. (1991), *Multicycle Slip Distribution along a Laboratory Fault*, Journal of Geophysical Research, Vol.96, No.B9. (pp. 14377 - 14381).

15. Kou B.C. (1987). *Automatic Control Systems*, 5 th edition, Prentice Hall, New Jersey. (pp. 96 - 98).

16. Mansur, W.J. & Brebbia, C.A. (1985), *Transient Elastodynamics*, Chapter 5 in *Topics in Boundary Element Research*, Vol.2, Time Dependant and Vibration Problems (C.A. Brebbia, Ed.), Springer-Verlag, berlin & New York.

17. Montgomery C.W. (1989), *Fundamentals of Geology*, 2 nd. Edition, Wm. C. Brown Publishers, Iowa. (pp. 138 142).

18. Ogata, K. (1978). *System Dynamics*, Prentice-Hall., New Jersey. (pp. 413 - 418) (pp. 424 - 431).

19. Phillips C.L. and Harbor R.D. (1996). *Feedback Control Systems*, Prentice Hall, New Jersey. (pp. 104 - 107).

20. Phillips C.L. (1995), *Digital Control System Analysis & Design*, 3 rd Edition, Prentice Hall, New Jersey. (pp. 111 - 113).

21. Rashid M.H. (1999), *Microelectronic Circuits, Analysis and Design*, P.W.S. Publishing Company, Boston. (pp. 283 - 288) (pp 292 - 295).

22. Raven, F.H. (1988). *Automatic Control Engineering*, Mc Graw-Hill, New York. (pp. 292-318).

23. Roberge J.K. (1981), *Operational Amplifiers*, John Wiley & Sons, New York. (pp. 502 - 525).

24. Sante, D.P. (1980). *Automatic Control System Technology*, Prentic-Hall, Inc., New Jersey. (pp. 72-73).

25. Schwarzenbach, J. and Gill, K.F. (1978). *System Modelling and Control*, Halsted Press, New York. (pp. 7) (pp. 28 - 57) (pp. 190).

26. Telford W.M., Geldart L.P., Sheriff R.E., Keys D.A. (1988), *Applied Geophysics*, Cambridge University Press, Cambridge. (pp. 228 - 246).

Appendix 1

Chaotic behavior of system as observed by Bajić

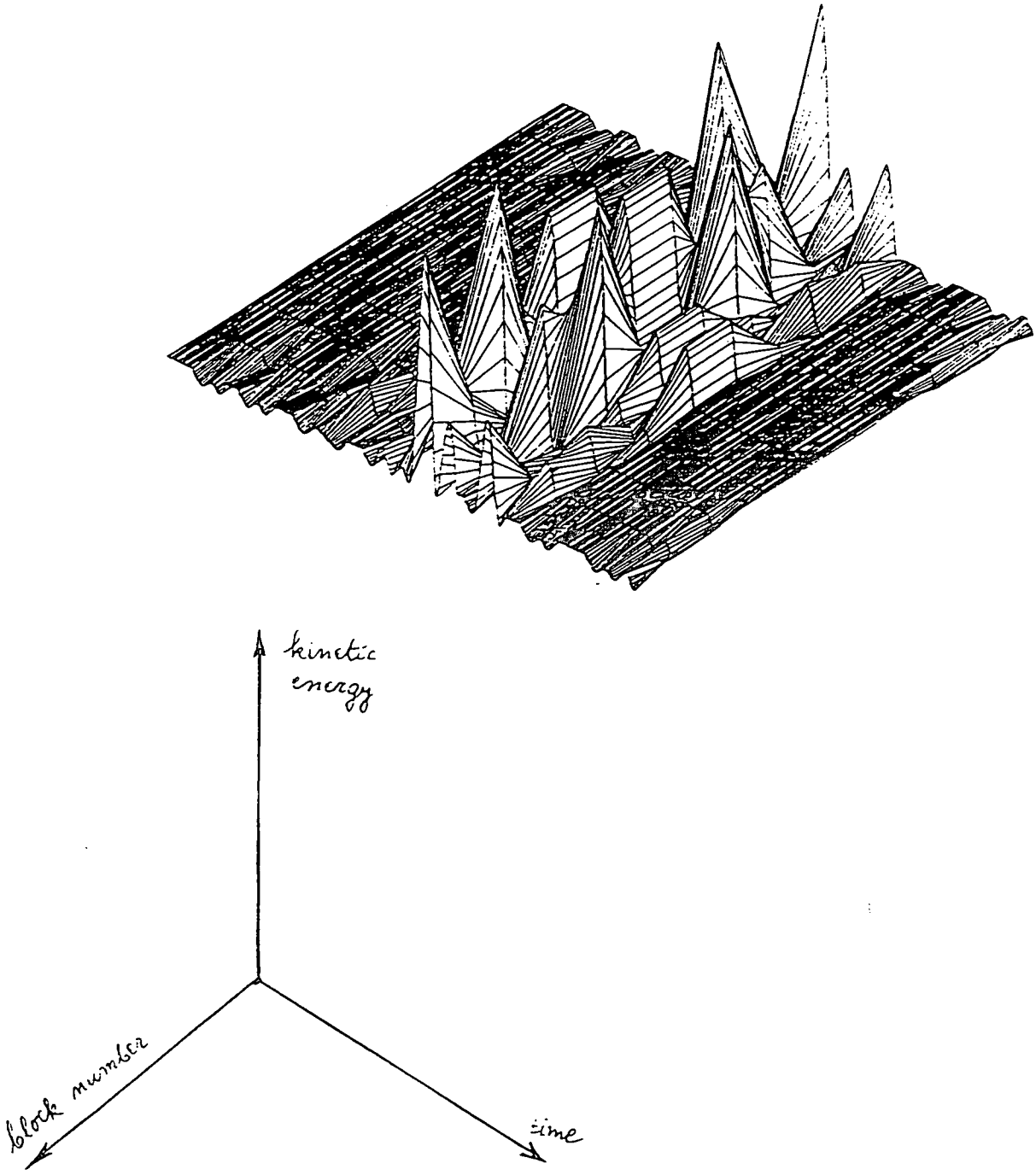

Fig. 7-0

"Chaotic" behavior of system

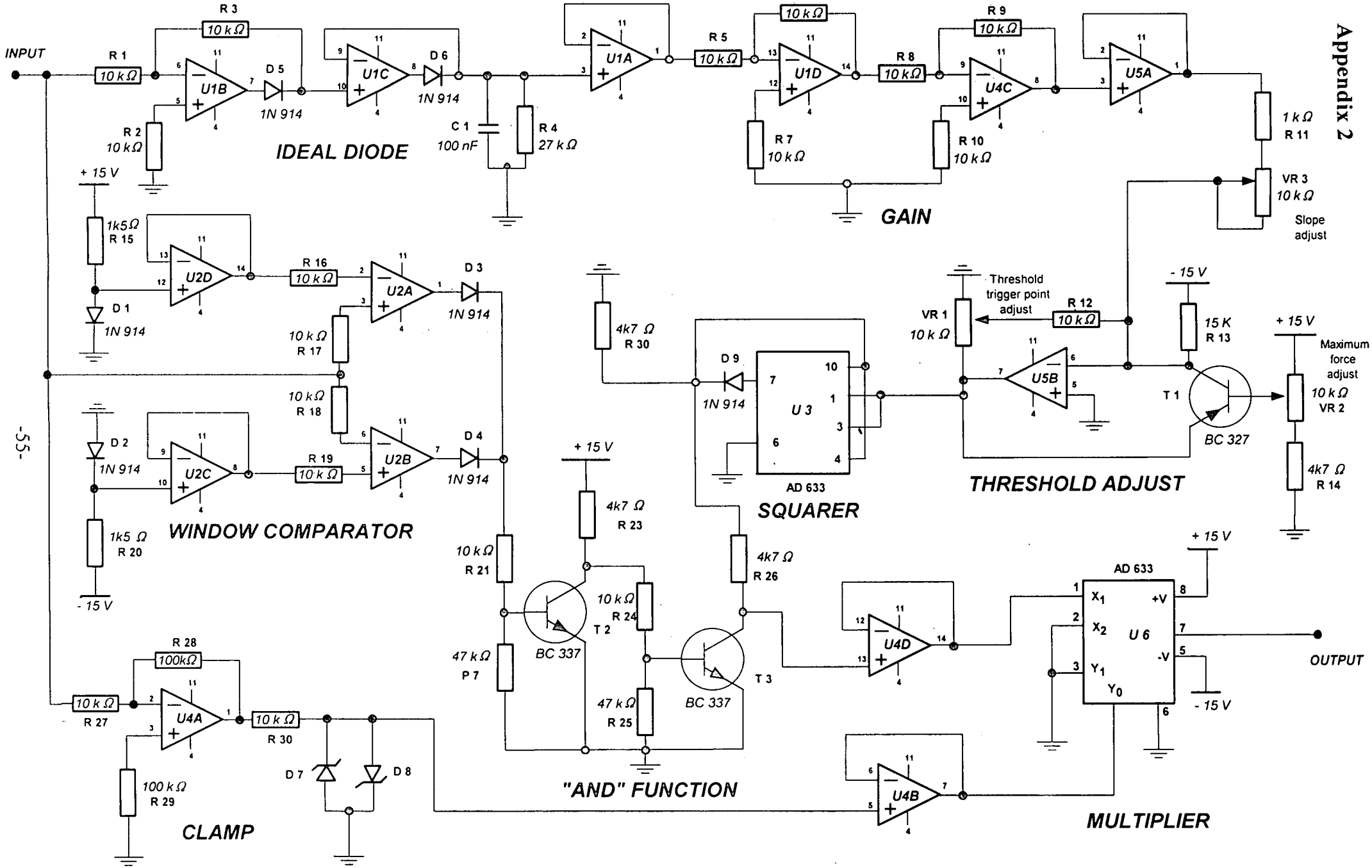

NON LINEAR CELL CIRCUIT DIAGRAM

Appendix 3 Master cell circuit diagram

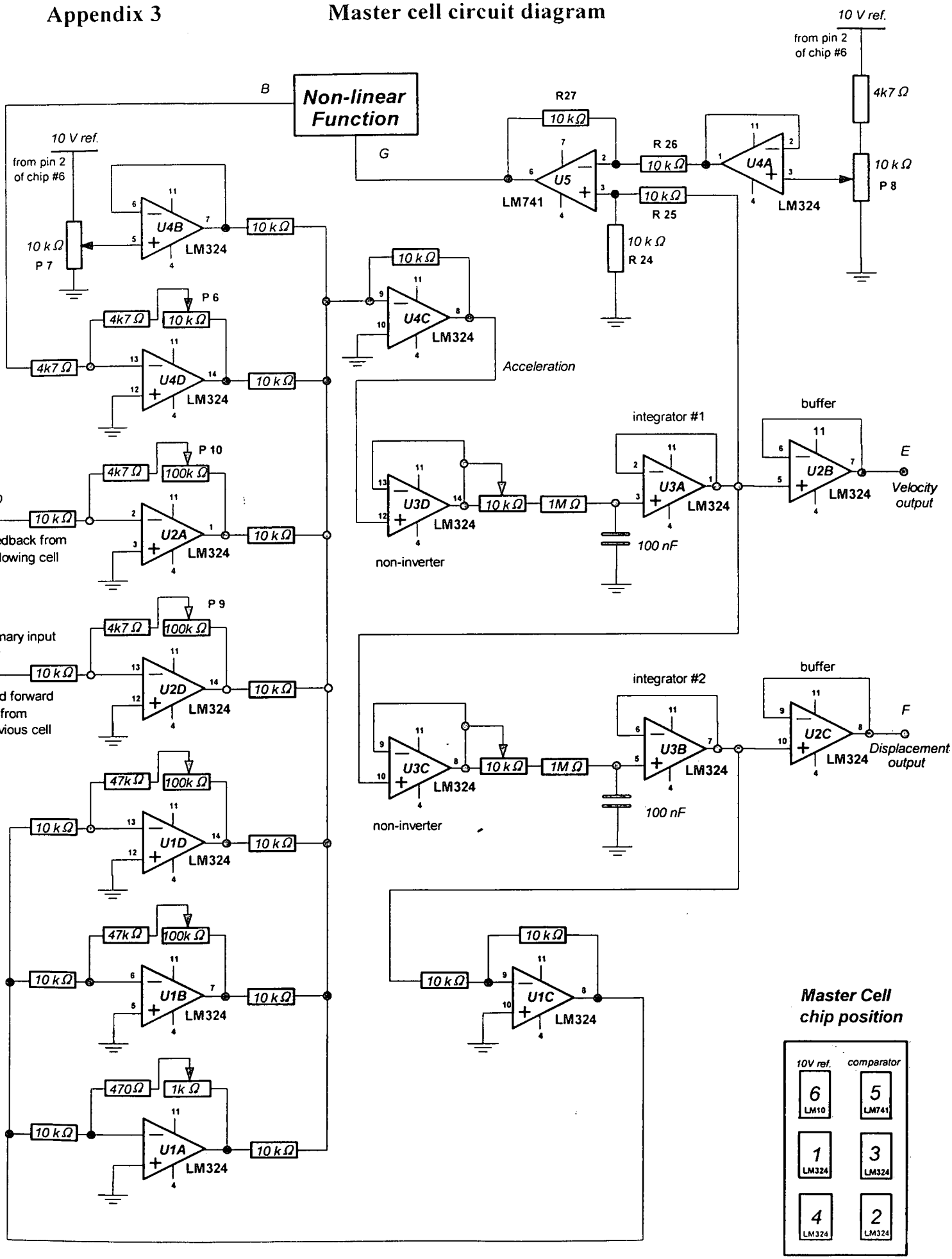

Appendix 4 Source code for A-D converter

```
program ADREAD4;

{errol3.pas}

uses dos,crt;

const

     b=$220;              {base address of card}

var

   hbyte,lbyte,chbyte,clbyte          :word;
   cnt,no_samples                     :integer;
   chan                               :integer;
   ha,ma,sa,sa100                     :word;
   hb,mb,sb,sb100                     :word;
   dtable                             :array[1..400,1..16] of
integer;
   ad_word                            :integer;
   chck_count                         :integer;
   pulse_width                        :integer;
   pulse_voltage                      :real;
   da_hi,da_lo                        :integer;


procedure get_no_samples;
{get number of samples required, width of pulse, from user}

begin

     repeat
          writeln('No. samples required (at 20/sec, 16 channel
s, MAX 400) ?');
          readln(no_samples);
     until no_samples<401;
     repeat
          writeln('Width of trigger pulse required (20 equiv.
to 1 sec) ?');
          readln(pulse_width);
     until pulse_width<401;

end;


procedure set_up_counters;
```

```
begin
     {2 MHz clock, require 20 Hz sample rate}
     {divide clock by 100 000, ie 1000 * 100}
     {both counters type 2}

     {write counter 1, 1000}

     port[b+3]:=116;  {counter 1 set up, 01 11 x10 0}

     port[b+1]:=232;  {lsb}
     port[b+1]:=3;    {msb}

     {write counter 2, 100}

     port[b+3]:=180;  {counter 2 set up}

     port[b+2]:=100;   {lsb}
     port[b+2]:=0;     {msb}

end;

procedure wait_for_counter;

begin

     {set trigger mode for counter trigger}
     port[b+11]:=3;


     repeat
     chbyte:=port[b+5];
     until chbyte<16;

     clbyte:=port[b+4];       {clear AD}

     {set trigger mode for software trigger}
     port[b+11]:=1;

end;

procedure send_DtoA;

begin

          if cnt>(10+pulse_width) then
```

```
          begin
               port[b+4]:=0;                {set A out}
               port[b+5]:=0;                {set A out}
               port[b+13]:=0;                {set D out}
               port[b+14]:=0;                {set D out}


          end

          else  if cnt>10 then
          begin
               port[b+4]:=0;
               port[b+5]:=0;
               port[b+13]:=255;              {set low byte D out}
               port[b+14]:=3;                {set high byte D out


          end

          else
          begin
               port[b+4]:=0;
               port[b+5]:=0;
               port[b+13]:=0;
               port[b+14]:=0;

          end

end;

procedure do_AD_reads;

begin

     {port[b+5]:=15;    D/A, timing point}

     chan:=0;

     repeat

     port[b+10]:=chan;

     port[b+12]:=0;    {software trigger}

          repeat
```

```
          hbyte:=port[b+5];
          until hbyte<16;

     lbyte:=port[b+4];

     ad_word:=(hbyte*256)+lbyte;

     dtable[cnt,chan+1]:= ad_word;

     inc (chan);
     until chan>15;

     {port[b+5]:=0      D/A, timing point}

end;

procedure dtable_to_file;

var
   dfile        :text;
   s_no,c_no    :integer;

begin
     assign(dfile,'c:\table.dat');
     rewrite (dfile);

   s_no:=1;

          repeat
                c_no:=1;

                     repeat
                           write(dfile,dtable[s_no,c_no]);
                           write(dfile,' ');        {space bet
ween samples}
                     inc(c_no);
                     until c_no>16;


          writeln(dfile);           {puts a return between each
 set}
          inc(s_no);
          until s_no>no_samples;

     close (dfile);
```

```
end;

procedure check_time;

var

   cntr_1_lsb,cntr_1_msb,cntr_2_lsb,cntr_2_msb      :word;
   cntr_1,cntr_2,elap_count                         :integer;

begin

     port[b+3]:=64;        {latch counter 1, 01 00 xxxx}
     port[b+3]:=128;       {latch counter 2, 10 00 xxxx}

     cntr_1_lsb:=port[b+1];
     cntr_1_msb:=port[b+1];

     cntr_2_lsb:=port[b+2];
     cntr_2_msb:=port[b+2];

     cntr_1:=(cntr_1_msb*256)+cntr_1_lsb;
     cntr_2:=(cntr_2_msb*256)+cntr_2_lsb;

     elap_count:=(100*cntr_1)+cntr_2;

     if chck_count<elap_count then chck_count:=elap_count;
end;


{MAIN BODY}

begin
     clrscr;

     get_no_samples;
     set_up_counters;

     gettime(ha,ma,sa,sa100);
     writeln('start time ',sa,'  ',sa100);

     chck_count:=0;

     cnt:=1;

          repeat
               wait_for_counter;
```

```
                send_DtoA;
                do_AD_reads;
                check_time;
                inc(cnt);

          until cnt > no_samples;

     gettime(hb,mb,sb,sb100);

     dtable_to_file;


     writeln('end time ',sb,'  ',sb100);

     writeln('count remaining  ',chck_count,' out of 100 000');

end.
```